NASA TECHNICAL NOTE

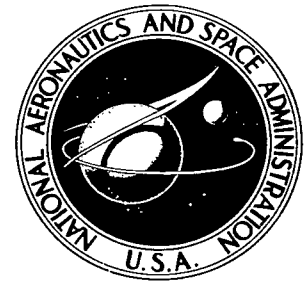

NASA TN D-8373

LOW-SPEED WIND-TUNNEL INVESTIGATION OF FLIGHT SPOILERS AS TRAILING-VORTEX-ALLEVIATION DEVICES ON AN EXTENDED-RANGE WIDE-BODY TRI-JET AIRPLANE MODEL

Delwin R. Croom, Raymond D. Vogler, and John A. Thelander

Langley Research Center
Hampton, Va. 23665

NATIONAL AERONAUTICS AND SPACE ADMINISTRATION • WASHINGTON, D. C. • DECEMBER 1976

1. Report No.	2. Government Accession No.	3. Recipient's Catalog No.
NASA TN D-8373		

4. Title and Subtitle	5. Report Date
LOW-SPEED WIND-TUNNEL INVESTIGATION OF FLIGHT SPOILERS AS TRAILING-VORTEX-ALLEVIATION DEVICES ON AN EXTENDED-RANGE WIDE-BODY TRI-JET AIRPLANE MODEL	December 1976
	6. Performing Organization Code
7. Author(s)	8. Performing Organization Report No.
Delwin R. Croom, Raymond D. Vogler, and John A. Thelander	L-11104
	10. Work Unit No. 514-52-01-03
9. Performing Organization Name and Address	11. Contract or Grant No.
NASA Langley Research Center Hampton, VA 23665	
	13. Type of Report and Period Covered
12. Sponsoring Agency Name and Address	Technical Note
National Aeronautics and Space Administration Washington, DC 20546	14. Sponsoring Agency Code

15. Supplementary Notes

Delwin R. Croom and Raymond D. Vogler: Langley Research Center.
John A. Thelander: Douglas Aircraft Company, McDonnell Douglas Corporation, Long Beach, California.

16. Abstract

An investigation was made in the Langley V/STOL tunnel to determine, by the trailing wing sensor technique, the effectiveness of various segments of the existing flight spoilers on an extended-range wide-body tri-jet transport airplane model when they were deflected as trailing-vortex-alleviation devices. On the transport model with the approach flap configuration, the four combinations of flight-spoiler segments investigated were effective in reducing the induced rolling moment on the trailing wing model by as much as 25 to 45 percent at downstream distances behind the transport model of 9.2 and 18.4 transport wing spans. On the transport airplane model with the landing flap configuration, the four combinations of flight-spoiler segments investigated were effective in reducing the induced rolling moment on the trailing wing model by as much as 35 to 60 percent at distances behind the transport model of from 3.7 to 18.4 transport wing spans, 18.4 spans being the downstream limit of distances used in this investigation.

17. Key Words (Suggested by Author(s))	18. Distribution Statement
Vortex alleviation Trailing-vortex hazard	Unclassified - Unlimited Subject Category 02

19. Security Classif. (of this report)	20. Security Classif. (of this page)	21. No. of Pages	22. Price*
Unclassified	Unclassified	52	$4.25

* For sale by the National Technical Information Service, Springfield, Virginia 22161

LOW-SPEED WIND-TUNNEL INVESTIGATION OF FLIGHT SPOILERS AS TRAILING-VORTEX-ALLEVIATION DEVICES ON AN EXTENDED-RANGE WIDE-BODY TRI-JET AIRPLANE MODEL

Delwin R. Croom, Raymond D. Vogler,
and John A. Thelander*
Langley Research Center

SUMMARY

An investigation was made in the Langley V/STOL tunnel to determine, by the trailing wing sensor technique, the effectiveness of various segments of the existing flight spoilers on an extended-range wide-body tri-jet transport airplane model when they were deflected as trailing-vortex-alleviation devices. On the transport model with the approach flap configuration, the four combinations of flight-spoiler segments investigated were effective in reducing the induced rolling moment on the trailing wing model by as much as 25 to 45 percent at downstream distances behind the transport model of 9.2 and 18.4 transport wing spans. On the transport airplane model with the landing flap configuration, the four combinations of flight-spoiler segments investigated were effective in reducing the induced rolling moment on the trailing wing model by as much as 35 to 60 percent at distances behind the transport model of from 3.7 to 18.4 transport wing spans, 18.4 spans being the downstream limit of distances used in this investigation.

INTRODUCTION

The strong vortex wakes generated by large transport airplanes are a potential hazard to smaller aircraft. The National Aeronautics and Space Administration is involved in a program of model tests, flight tests, and theoretical studies to determine the feasibility of reducing this hazard by aerodynamic means.

Results of recent investigations have indicated that the trailing vortex behind an unswept-wing model (ref. 1) or a swept-wing transport model (ref. 2) can be attenuated by a forward-mounted spoiler. It was also determined by model tests (ref. 3) and verified in full-scale flight tests (ref. 4) that there are several combinations of the existing flight-spoiler segments on the jumbo-jet airplane that are effective as trailing-vortex-alleviation devices. The approach used in references 1, 2, and 3 to evaluate the effectiveness of vortex-alleviation devices was to simulate an airplane flying in the trailing vortex of another larger airplane and to make direct measurements of rolling moments induced on the trailing model by the vortex

*Douglas Aircraft Company, McDonnell Douglas Corporation, Long Beach, California.

generated by the forward model. The technique used in the full-scale flight tests was to penetrate the trailing vortex wake behind a Boeing 747 airplane with a Cessna T-37 airplane and to evaluate the roll attitude and roll rate of the Cessna T-37 airplane as an index to the severity of the trailing-vortex encounter.

The purpose of the present investigation was to determine the trailing-vortex-alleviation effectiveness of various segments of the existing flight spoiler on an extended-range wide-body tri-jet transport airplane model. The direct-measurement technique described in references 1, 2, and 3 was used with the trailing wing model from 3.7 to 18.4 transport wing spans behind the transport model. (For the full-scale transport airplane, this would represent a range of downstream distance from 0.1 to 0.5 nautical mile.)

SYMBOLS

All data are referenced to the wind axes. The pitching-moment coefficients are referenced to the quarter-chord of the wing mean aerodynamic chord.

b wing span, m

C_D drag coefficient, $\frac{\text{Drag}}{qS_W}$

C_L lift coefficient, $\frac{\text{Lift}}{qS_W}$

$C_{l,TW}$ trailing wing rolling-moment coefficient, $\frac{\text{Trailing wing rolling moment}}{qS_{TW}b_{TW}}$

C_m pitching-moment coefficient, $\frac{\text{Pitching moment}}{qS_W\bar{c}_W}$

c wing chord, m

$\bar{c}$ wing mean aerodynamic chord, m

i_t horizontal-tail incidence, referred to fuselage reference line (positive direction trailing edge down), deg

l longitudinal distance in tunnel diffuser, m

q dynamic pressure, Pa

S wing area, m^2

X',Y',Z' system of axes originating at left wing tip of transport airplane model (see fig. 1)

x', y', z' longitudinal, lateral, and vertical dimensions measured from trailing edge of left wing tip of transport airplane model, m

$\Delta y', \Delta z'$ incremental dimensions along Y'- and Z'-axes, m

α angle of attack of fuselage reference line, deg (wing root incidence is 3° relative to fuselage reference line)

δ deflection, deg

ϕ local streamline angle in tunnel diffuser relative to tunnel center line, deg

Subscripts:

flap transport airplane model flap

max maximum

slat transport airplane model slat

spoiler transport airplane model spoiler

TW trailing wing model

W transport airplane model

MODEL AND APPARATUS

A three-view sketch and principal geometric characteristics of the 0.047-scale model of an extended-range wide-body commercial tri-jet transport airplane (McDonnell Douglas DC-10-30) are shown in figure 1. Sketches of the landing and approach flap configurations are shown in figures 2 and 3, respectively. Figure 4 is a photograph of the transport model mounted in the Langley V/STOL tunnel. Figure 5 is a sketch showing the location of the flight spoilers on the transport model. Photographs of the four combinations of flight-spoiler segments investigated are presented in figure 6. Spoiler segments 1 and 2 (fig. 6(a)) and 3 and 4 (fig. 6(c)) were deflected as units by internal electrical motors. No provision was made in the model to deflect the segments separately; therefore, spoiler segments 2 and 3 (fig. 6(b)) and 1 and 4 (fig. 6(d)) were simulated with wedges.

The test section of the Langley V/STOL tunnel has a height of 4.42 m, a width of 6.63 m, and a length of 14.24 m. The transport model was strut supported on a six-component strain-gage balance system which measured the forces and moments. The angle of attack was determined from an accelerometer mounted in the fuselage.

A photograph and dimensions of the unswept trailing wing model installed on a traverse mechanism are presented in figure 7. The trailing model has a span and aspect ratio typical of small-size transport airplanes. It was

mounted on a single-component strain-gage roll balance, which was attached to the traverse mechanism capable of moving the model both laterally and vertically. (See fig. 7.) The lateral and vertical positions of the trailing model were measured by outputs from digital encoders. This entire traverse mechanism could be mounted to the tunnel floor at various tunnel longitudinal positions downstream of the transport airplane model.

TESTS AND CORRECTIONS

Transport Airplane Model

All tests were made at a free-stream dynamic pressure (in the tunnel test section) of 430.9 Pa which corresponds to a velocity of 27.4 m/sec. The Reynolds number for these tests was approximately 6.4×10^5 based on the wing mean aerodynamic chord. No transition grit was applied to the transport airplane model. The basic longitudinal aerodynamic characteristics were obtained through an angle-of-attack range of approximately -4° to 22°. All tests were made with the leading-edge devices extended. The landing gear was retracted for the approach flap configuration and was extended for the landing flap configuration.

Blockage corrections were applied to the data by the method of reference 5. Jet-boundary corrections to the angle of attack and the drag were applied in accordance with reference 6. No corrections were applied to the data for any possible strut interference effects.

Trailing Wing Model

The trailing wing model and its associated roll-balance system were used as a sensor to measure the induced rolling moment caused by the vortex flow downstream of the transport airplane model. No transition grit was applied to the trailing model. The trailing model was positioned at a given distance downstream of the transport model on the traverse mechanism which was positioned laterally and vertically so that the trailing vortex was near the center of the mechanism. The trailing vortex was probed with the trailing model. A large number of trailing wing rolling-moment data points (usually from 50 to 100) were obtained from the lateral traverses at several vertical locations to insure good definition of the vortex wake. In addition, certain test conditions were repeated at selected intervals during the test period and the data were found to be repeatable.

Trailing wing rolling-moment measurements were made at downstream scale distances from about 3.7 to 18.4 transport wing spans behind the transport airplane model. All trailing wing rolling-moment data at distances downstream greater than about 3.7 spans were obtained with the trailing model positioned in the diffuser section of the V/STOL tunnel. These data were reduced to coefficient form based on the dynamic pressure at the trailing wing location. For these tests, the dynamic pressures at the 3.69, 9.19, and 18.39 span locations were 430.9, 253.1, and 85.5 Pa, respectively. The trailing wing location relative to the wing tip of the transport model has been

corrected to account for the progressively larger tunnel cross-sectional area in the diffuser section. The corrections to the trailing wing location in the diffuser were made by assuming that the local streamline angles in the tunnel diffuser section are equal to the ratio of the distance from the tunnel center line to the local tunnel half-width or half-height multiplied by the diffuser half-angle. Corrections to the trailing model locations are as follows: $\Delta y'$ correction or $\Delta z'$ correction $= l \tan \phi$ where $\Delta y'$ correction and $\Delta z'$ correction are, respectively, the corrections to the measured lateral and vertical locations of the trailing model relative to the left wing tip of the transport airplane model, l is the longitudinal distance in the tunnel diffuser, and ϕ is the local streamline angle in the tunnel diffuser relative to the tunnel center line.

RESULTS AND DISCUSSION

Transport Airplane Model

The longitudinal aerodynamic characteristics of the transport airplane model with the double-slotted flaps and leading-edge slats in the landing configuration (see fig. 2) and in the approach configuration (see fig. 3) are presented in figures 8 and 9, respectively. These data were obtained with the horizontal tail off and over a range of horizontal-tail incidence sufficient to trim the model throughout the range of lift coefficient. These data indicate that the transport model with either flap configuration was statically stable up to the stall. The static margin, $\partial C_m/\partial C_L$, for the model with either flap configuration was about -0.24.

The longitudinal aerodynamic characteristics of the transport model with flight-spoiler segments 1 and 2, 2 and 3, 3 and 4, and 1 and 4 deflected symmetrically through a spoiler deflection range of from 0° to 60° are presented in figures 10, 11, 12, and 13, respectively, for the landing flap configuration and in figures 14, 15, 16, and 17, respectively, for the approach flap configuration. For any one of these configurations, there is essentially a linear increase in drag with spoiler deflection. For the landing flap configuration, about 50 percent of the lift loss at a given angle of attack occurred at a spoiler deflection of only 15°; whereas for the approach flap configuration, about 50 percent of the lift loss at a given angle of attack occurred at a spoiler deflection of about 30°. For both flap configurations, the variation of pitching-moment coefficient with angle of attack was more linear when the spoilers were deflected than when they were retracted.

The longitudinal aerodynamic characteristics of the transport airplane model with the four combinations of the flight-spoiler segments (1 and 2, 2 and 3, 3 and 4, and 1 and 4) on each wing deflected symmetrically 45° are presented in figures 18 and 19 for the landing flap configuration and the approach flap configuration, respectively. These data indicate that a nominal lift coefficient for approach of about 1.2 can be maintained with an angle-of-attack increase of about 3.5° for the landing flap configuration and of about 2° for the approach flap configuration when any combination of flight spoilers investigated was deflected 45°. It can also be seen in figures 18 and 19 that the maximum increase in drag due to spoiler (at

C_L = 1.2) for any of the spoiler combinations is of the order of 0.04, and that the maximum lift coefficient was reduced due to spoiler by as much as 0.23 for the landing flap configuration and by as much as 0.06 for the approach flap configuration. These results also indicate that the static margin $\partial C_m/\partial C_L$ was reduced due to spoiler by as much as 0.04 for the landing flap configuration and by as much as 0.05 for the approach flap configuration.

Trailing Wing Model

Flight-spoiler segments 1 and 2, and 3 and 4 and flight-spoiler segments 2 and 3, and 1 and 4 simulated with wedges were tested on the transport airplane model with the approach flap configuration and with the landing flap configuration over a spoiler deflection range from 0° to 60° with the trailing wing model positioned 3.7, 9.2, and 18.4 transport wing spans behind the transport model. The maximum rolling-moment coefficient measured by the trailing wing model and the position of this model relative to the left wing tip of the transport airplane model are presented as a function of flight-spoiler deflection in figure 20 for the approach flap configuration and in figures 21 and 22 for the landing flap configuration.

The trailing wing rolling-moment data obtained at 3.7 spans downstream of the approach flap configuration (fig. 20(a)) indicate that the trailing-vortex system may not be fully developed since the spoiler-retracted data seem to be quite low and the flight spoilers were not effective. At all other downstream distances investigated behind the approach flap configuration (figs. 20(b) and 20(c)) and at all downstream distances investigated behind the landing flap configuration (figs. 21 and 22), all the spoiler combinations investigated were effective. These data (figs. 20(b), 20(c), 21, and 22) show that generally the induced rolling moment on the trailing model decreased with increase in both downstream distance and spoiler deflection.

Figure 22 shows results obtained with the actual flight-spoiler segments 1 and 2, and 3 and 4 and with flight-spoiler segments 1 and 2, and 3 and 4 simulated with wedges. These data indicate that the effectiveness of spoiler segments simulated with wedges is slightly less than that obtained with the actual flight spoilers. Therefore, the results obtained with flight-spoiler segments 2 and 3, and 1 and 4 simulated with wedges may be conservative.

The maximum rolling-moment coefficient measured by the trailing wing model and the position of this model relative to the left wing tip of the transport model are presented as a function of downstream distance in figure 23 for the approach flap configuration and the landing flap configuration. For any spoiler configuration tested, most of the reduction in induced rolling moment on the trailing model was realized with about 45° of spoiler deflection (figs. 20 to 22). For this reason, these measurements (fig. 23) were made with the flight spoilers retracted and with various segments of the flight spoilers deflected 45°.

It can be seen in figure 23 that all combinations of flight spoilers investigated were effective in reducing the induced rolling moment on the trailing model for the approach flap configuration at downstream distances of 9.19 and 18.39 spans and for the landing flap configuration at all downstream distances investigated. The largest reduction in induced rolling moment for the approach flap configuration was realized with spoiler segments 2 and 3 (reductions in $(C_{l,TW})_{max}$ of the order of 40 percent), whereas the largest reduction for the landing flap configuration was realized with spoiler segments 3 and 4 (reductions in $(C_{l,TW})_{max}$ of the order of 60 percent). It is interesting to note that for the landing flap configuration, a large reduction in $(C_{l,TW})_{max}$ (35 to 50 percent) was realized in a relatively near distance (about 4 transport wing spans) downstream of the transport airplane model (fig. 23(b)). For the approach flap configuration (fig. 23(a)), reductions in $(C_{l,TW})_{max}$ were not realized until the trailing model was located farther than 4 wing spans downstream of the transport model. At the downstream location of 9.2 wing spans, reductions in $(C_{l,TW})_{max}$ of the order of 25 to 45 percent were realized (fig. 23(a)).

The attenuated values of $(C_{l,TW})_{max}$ obtained with flight-spoiler segments 3 and 4 on the present extended-range tri-jet transport airplane model in the landing flap configuration (fig. 23(b)) are comparable with the attenuated values of $(C_{l,TW})_{max}$ obtained in previous wind-tunnel tests (see ref. 3) of the jumbo-jet transport airplane model in its landing flap configuration. Flight spoilers were shown to be effective in attenuating the trailing vortex in full-scale flight tests of the jumbo-jet transport airplane (ref. 4); therefore, it appears that the flight spoilers on the present extended-range tri-jet transport airplane would also be effective in attenuating the trailing vortex behind this airplane.

SUMMARY OF RESULTS

Results have been presented of an investigation in the Langley V/STOL tunnel to determine, by the trailing wing sensor technique, the trailing-vortex-alleviation effectiveness of various segments of the flight spoilers on an extended-range tri-jet transport airplane model when the segments are deflected as trailing-vortex-alleviation devices.

On the transport airplane model with the landing flap configuration, the four combinations of flight-spoiler segments investigated were all effective in reducing the induced rolling moment on the trailing wing model by as much as 35 to 60 percent throughout the range of downstream distance used in this investigation. The largest reduction was realized with the two innermost spoiler segments investigated (segments 3 and 4).

On the transport airplane model with the approach flap configuration, the four combinations of flight-spoiler segments investigated were all effective in reducing the induced rolling moment on the trailing wing model by as much as 25 to 45 percent at downstream distances of 9.2 and 18.4 transport

wing spans. The largest reduction was realized with the middle two spoiler segments investigated (segments 2 and 3).

Langley Research Center
National Aeronautics and Space Administration
Hampton, VA 23665
November 23, 1976

REFERENCES

1. Croom, Delwin R.: Low-Speed Wind-Tunnel Investigation of Forward-Located Spoilers and Trailing Splines as Trailing-Vortex Hazard-Alleviation Devices on an Aspect-Ratio-8 Wing Model. NASA TM X-3166, 1975.

2. Croom, Delwin R.; and Dunham, R. Earl, Jr.: Low-Speed Wind-Tunnel Investigation of Span Load Alteration, Forward-Located Spoilers, and Splines as Trailing-Vortex-Hazard Alleviation Devices on a Transport Aircraft Model. NASA TN D-8133, 1975.

3. Croom, Delwin R.: Low-Speed Wind-Tunnel Investigation of Various Segments of Flight Spoilers as Trailing-Vortex-Alleviation Devices on a Transport Aircraft Model. NASA TN D-8162, 1976.

4. Barber, Marvin R.; Hastings, Earl C., Jr.; Champine, Robert A.; and Tymczyszyn, Joseph J.: Vortex Attenuation Flight Experiments. Wake Vortex Minimization, NASA SP-409, 1976.

5. Herriot, John G.: Blockage Corrections for Three-Dimensional-Flow Closed-Throat Wind Tunnels, With Consideration of the Effect of Compressibility. NACA Rep. 995, 1950. (Supersedes NACA RM A7B28.)

6. Gillis, Clarence L.; Polhamus, Edward C.; and Gray, Joseph L., Jr.: Charts for Determining Jet-Boundary Corrections for Complete Models in 7- by 10-Foot Closed Rectangular Wind Tunnels. NACA WR L-123, 1945. (Formerly NACA ARR L5G31.)

WING	
Span, m	2.369
Mean aerodynamic chord, m	0.353
Sweepback at quarter-chord, deg	35
Area, m^2	0.7486
Aspect ratio	7.498
Taper ratio	0.254
FUSELAGE	
Length, m	2.442
HORIZONTAL TAIL	
Span, m	1.020
Area, m^2	0.2746
Aspect ratio	3.787

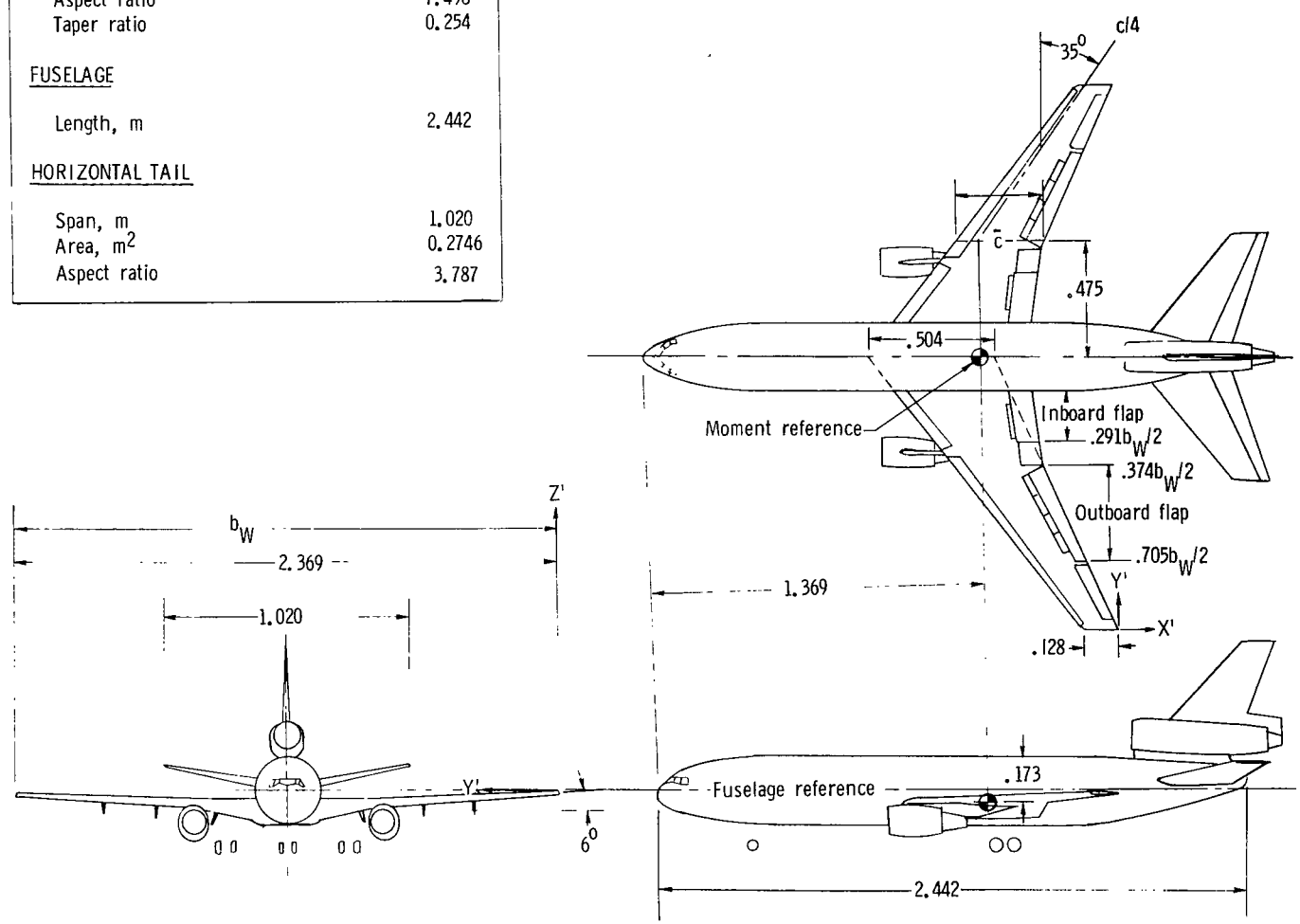

Figure 1.- Three-view sketch of transport model with flaps retracted. Linear dimensions are in meters.

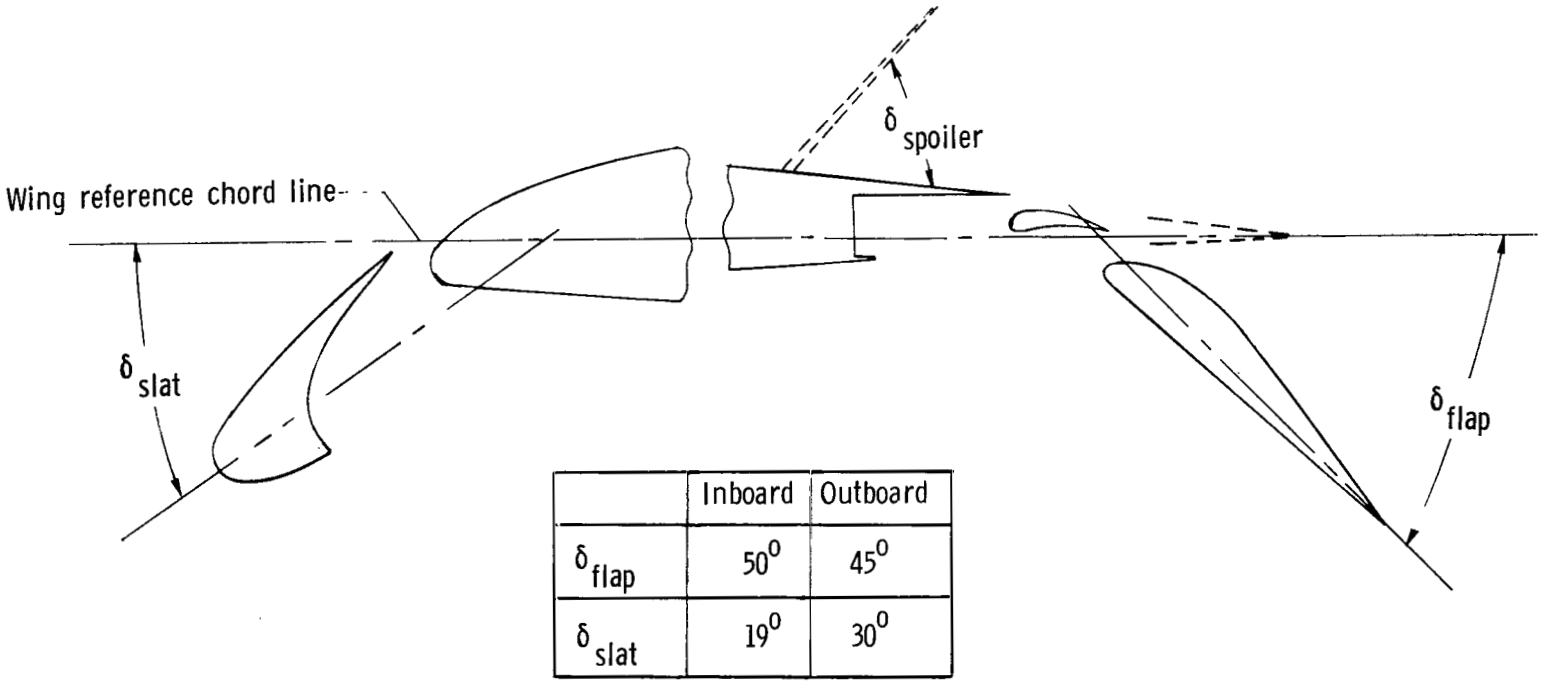

	Inboard	Outboard
δ_{flap}	50^0	45^0
δ_{slat}	19^0	30^0

Figure 2.- Sketch of spoiler and high-lift devices for landing configuration.

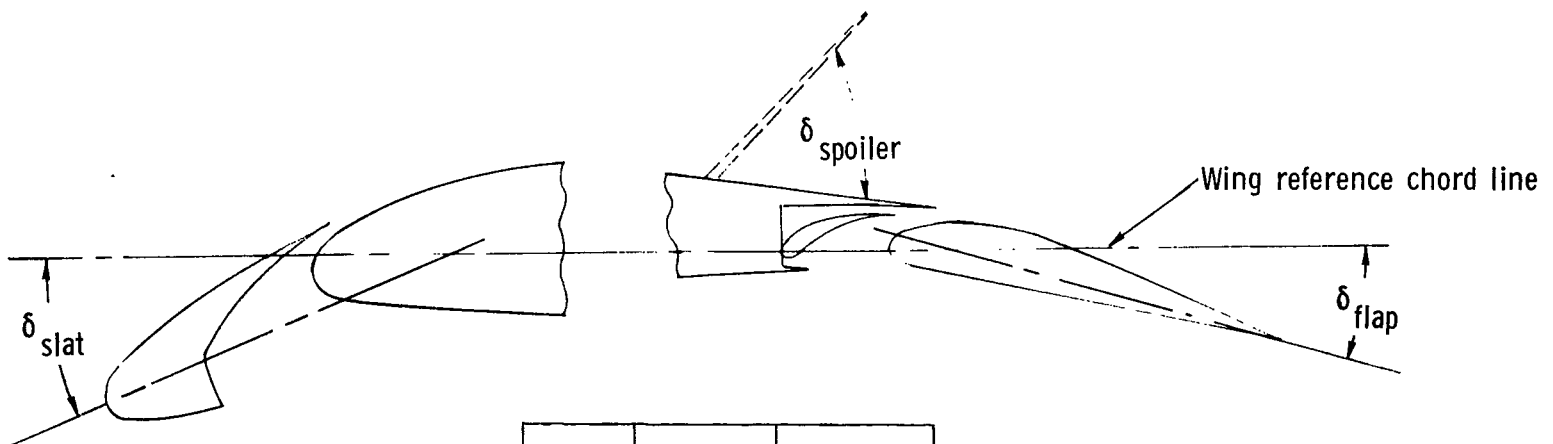

	Inboard	Outboard
δ_{flap}	25^0	22^0
δ_{slat}	15^0	25^0

Figure 3.- Sketch of spoiler and high-lift devices for approach configuration.

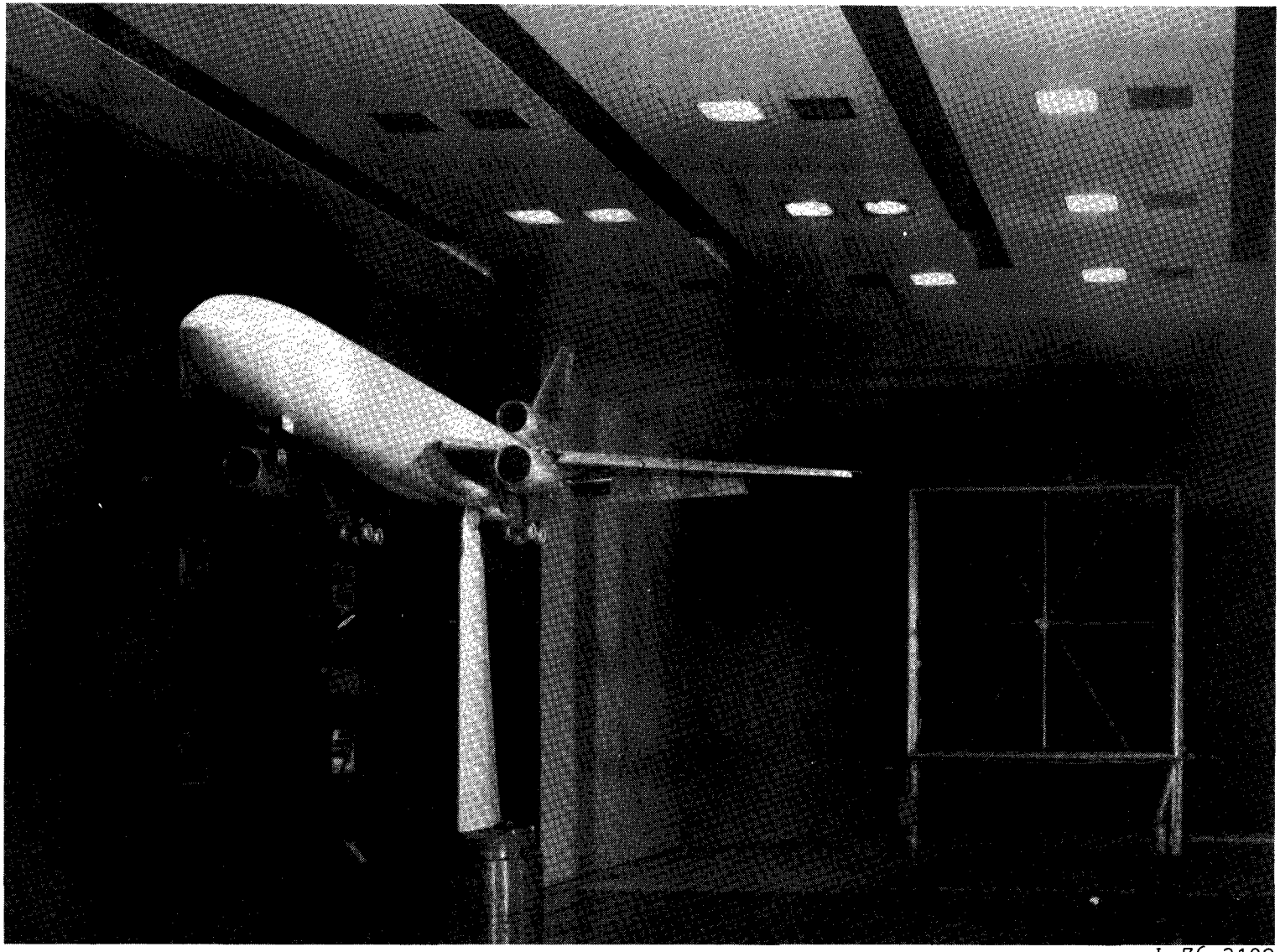

L-76-3102

Figure 4.- Photograph of test setup in Langley V/STOL tunnel. Transport airplane model in landing flap configuration.

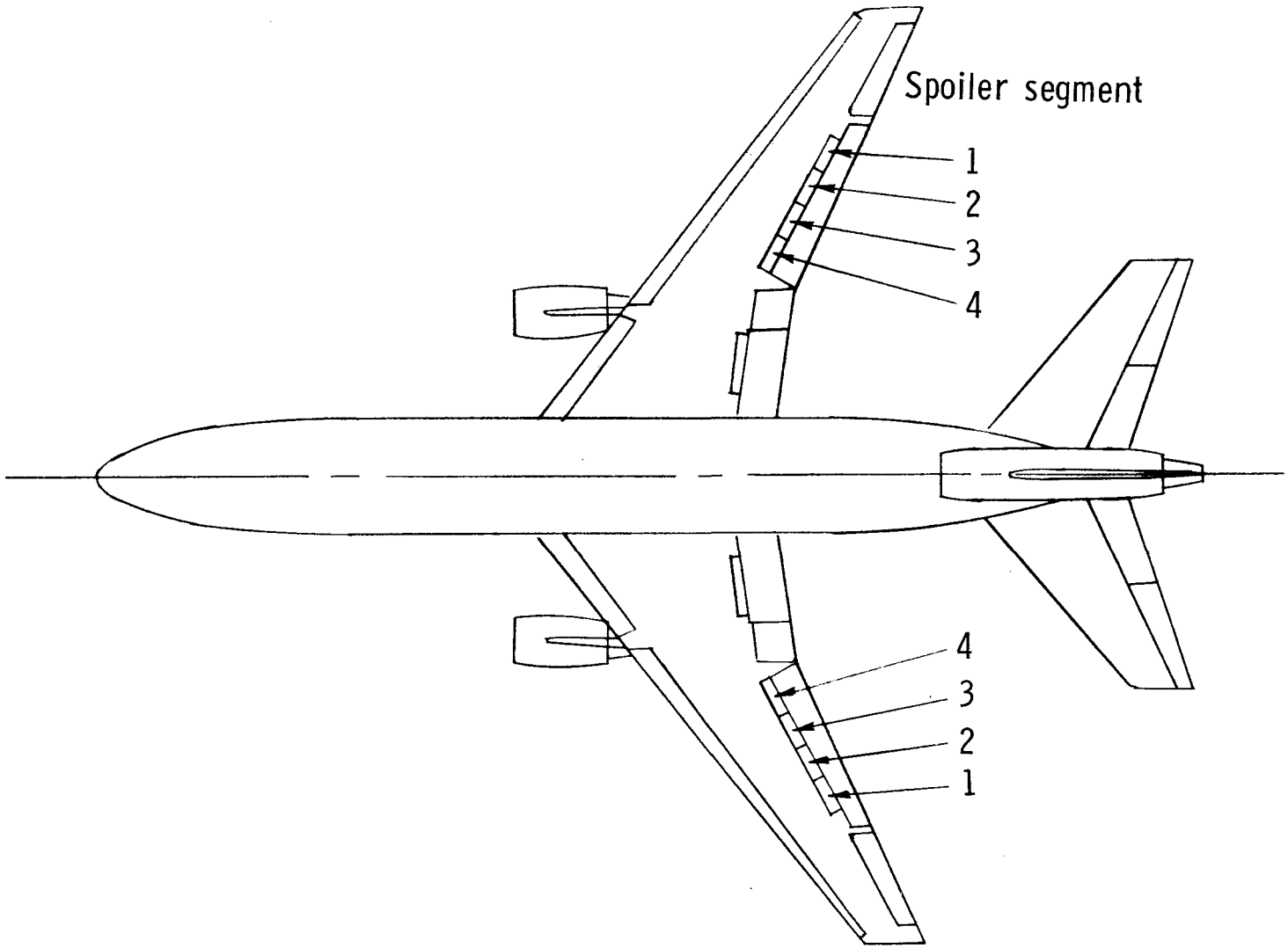

Figure 5.- Sketch of flight spoilers on transport airplane model.

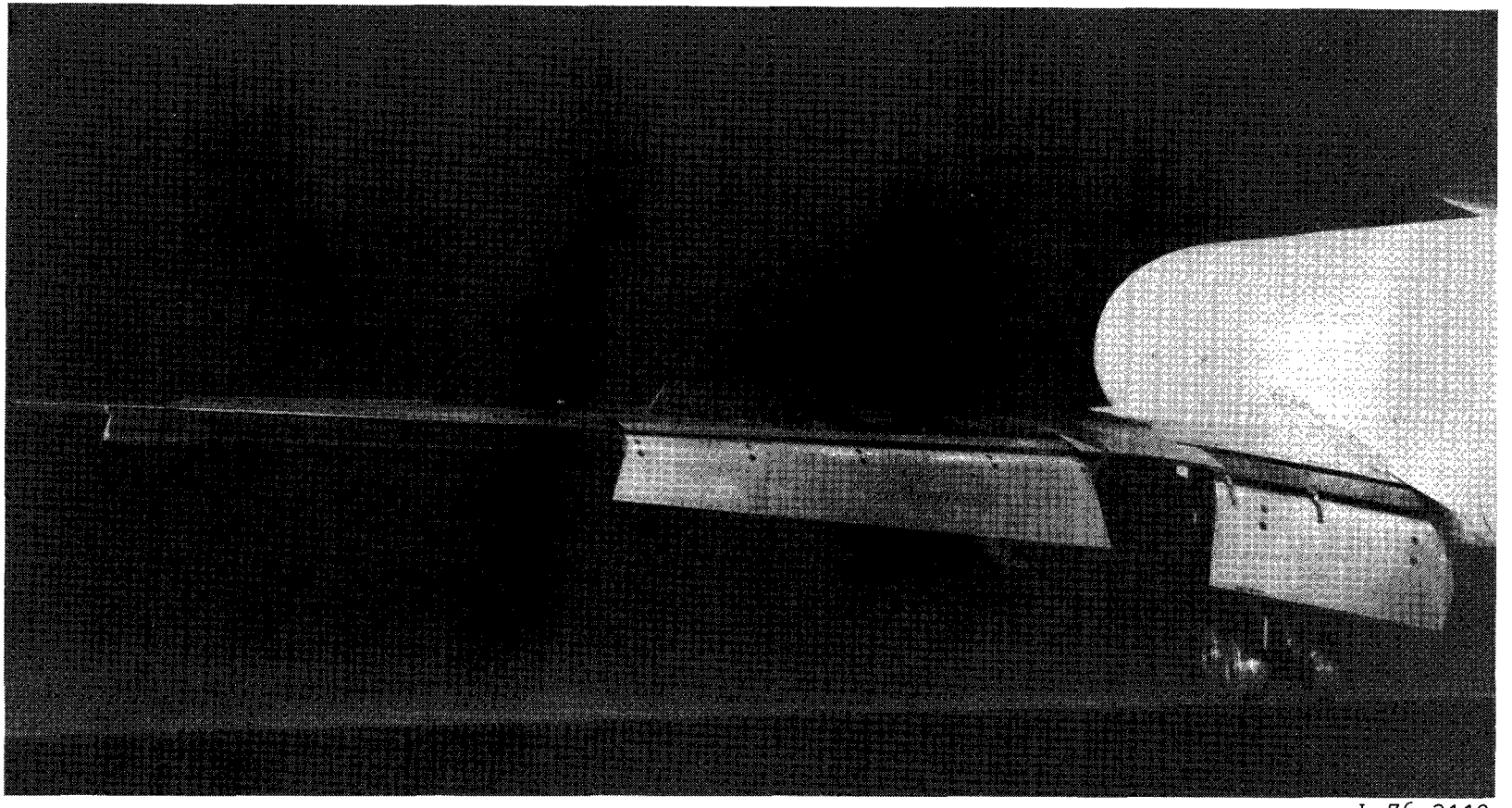

L-76-3119

(a) Spoiler segments 1 and 2 deflected 45°.

Figure 6.- Photographs of flight spoilers on transport airplane model.

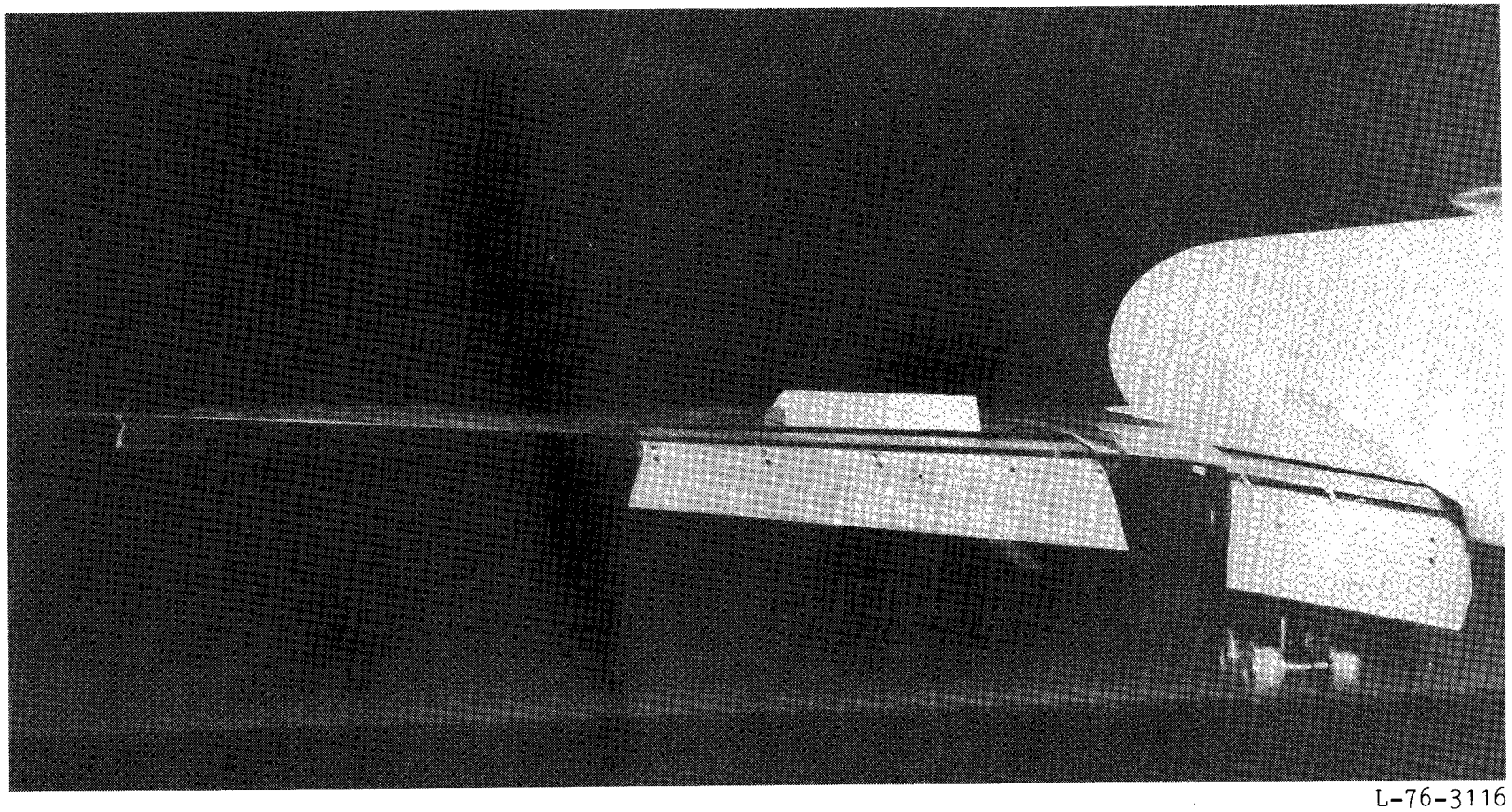

L-76-3116

(b) Spoiler segments 2 and 3 deflected 45°. Segments simulated with wedges.

Figure 6.- Continued.

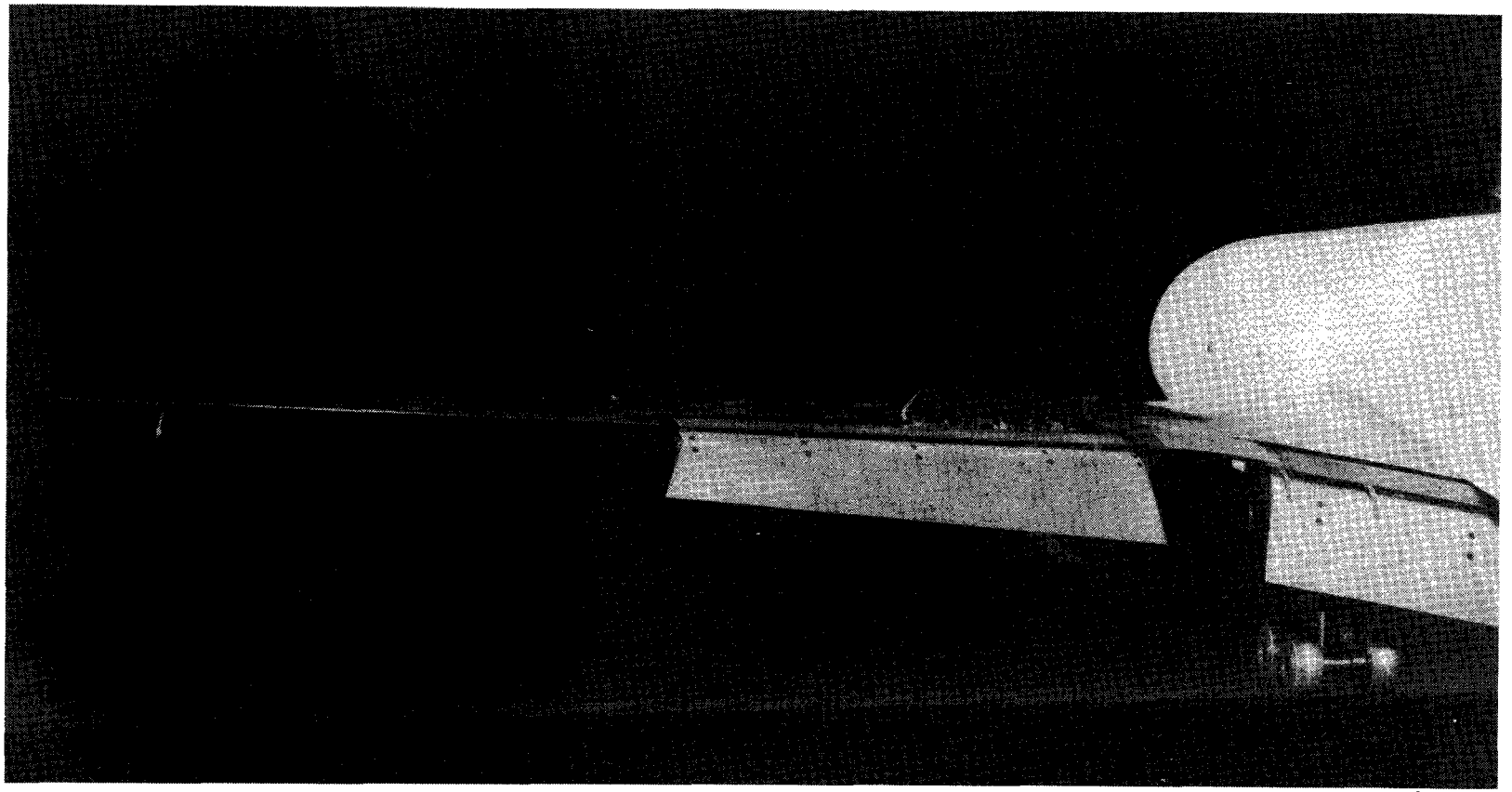

L-76-3117

(c) Spoiler segments 3 and 4 deflected 45°.

Figure 6.- Continued.

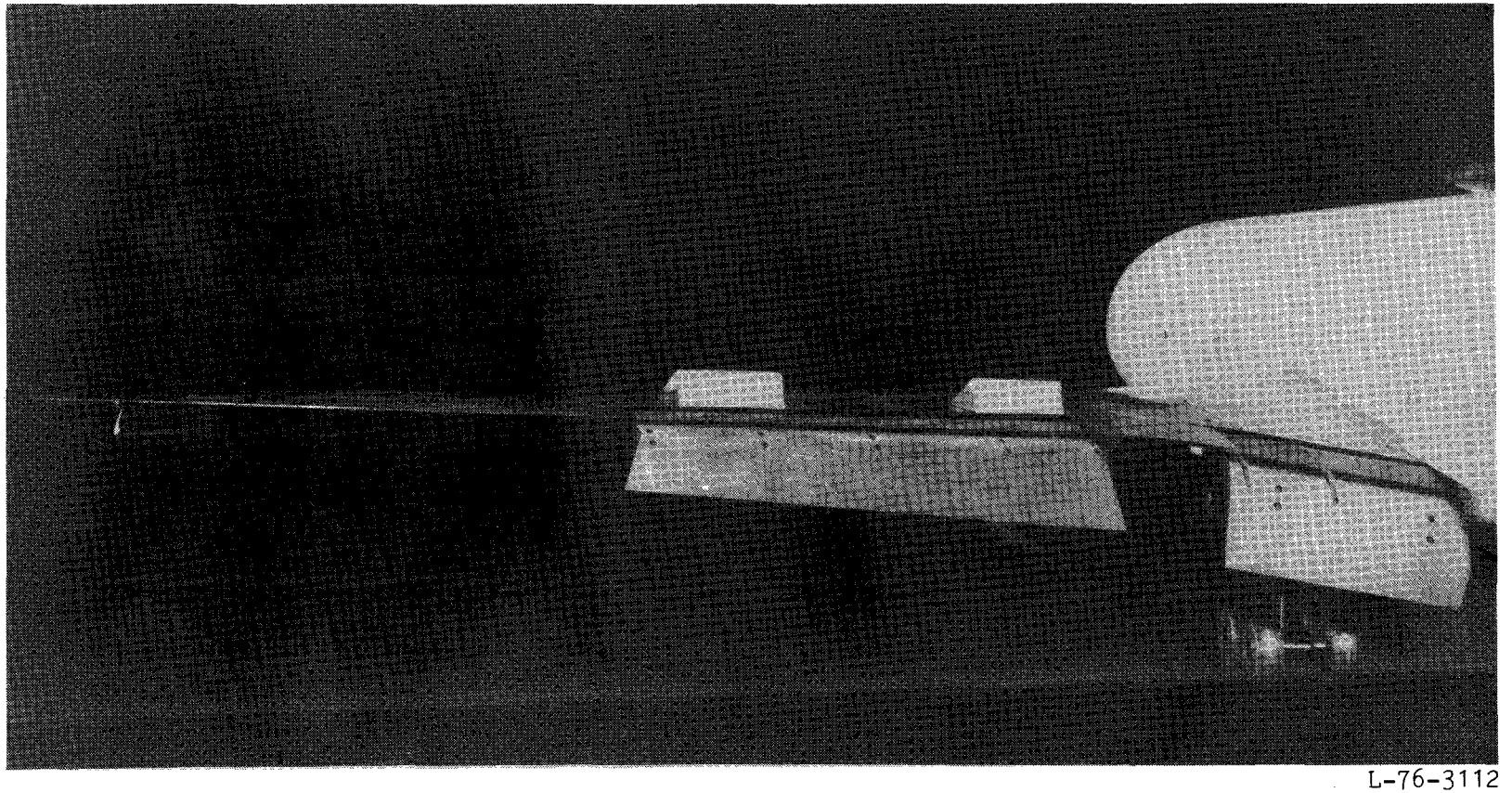

L-76-3112

(d) Spoiler segments 1 and 4 deflected 45°. Segments simulated with wedges.

Figure 6.- Concluded.

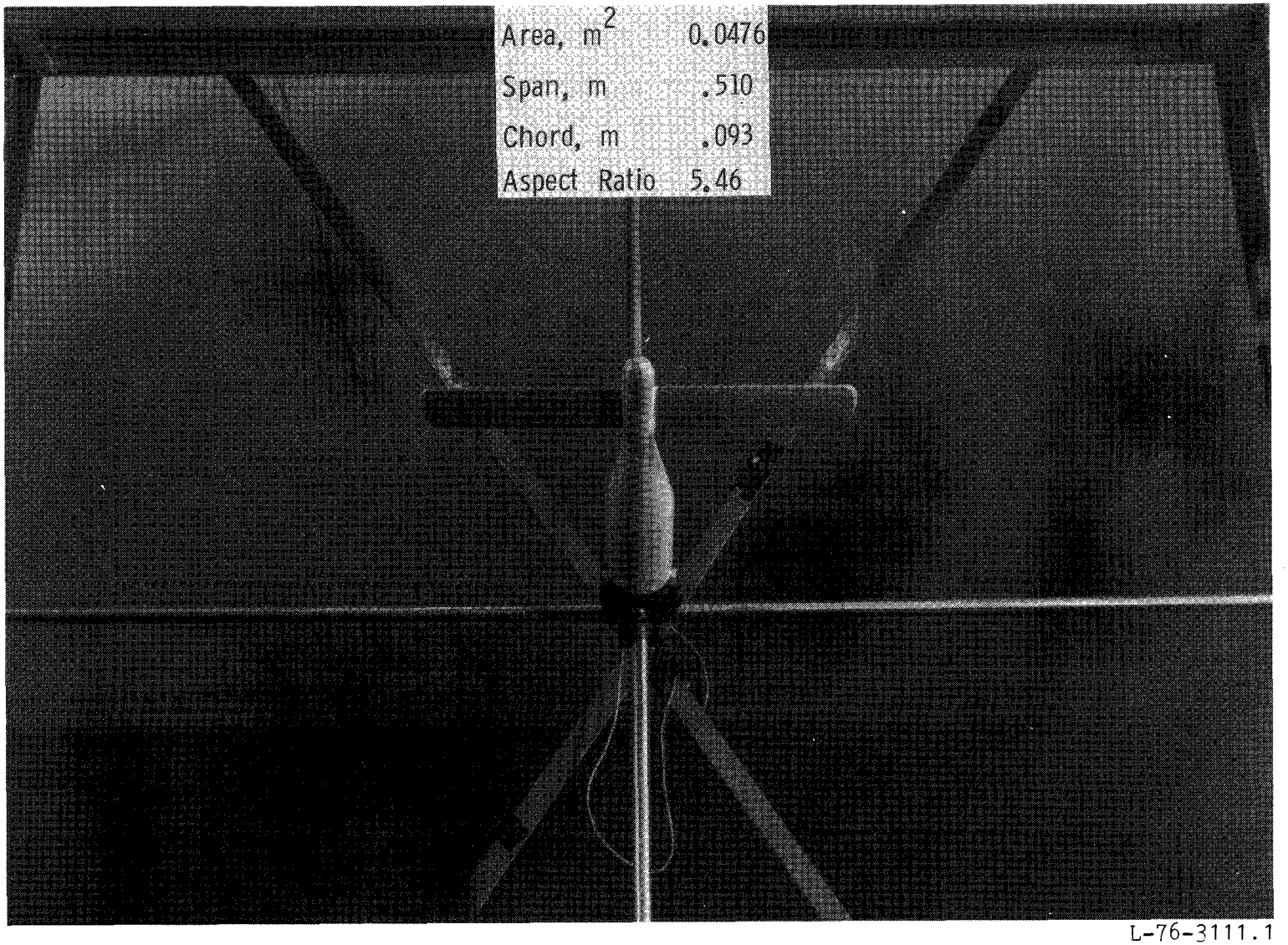

L-76-3111.1

Figure 7.- Photograph and dimensions of unswept trailing wing model on traverse mechanism. Model has NACA 0012 airfoil section.

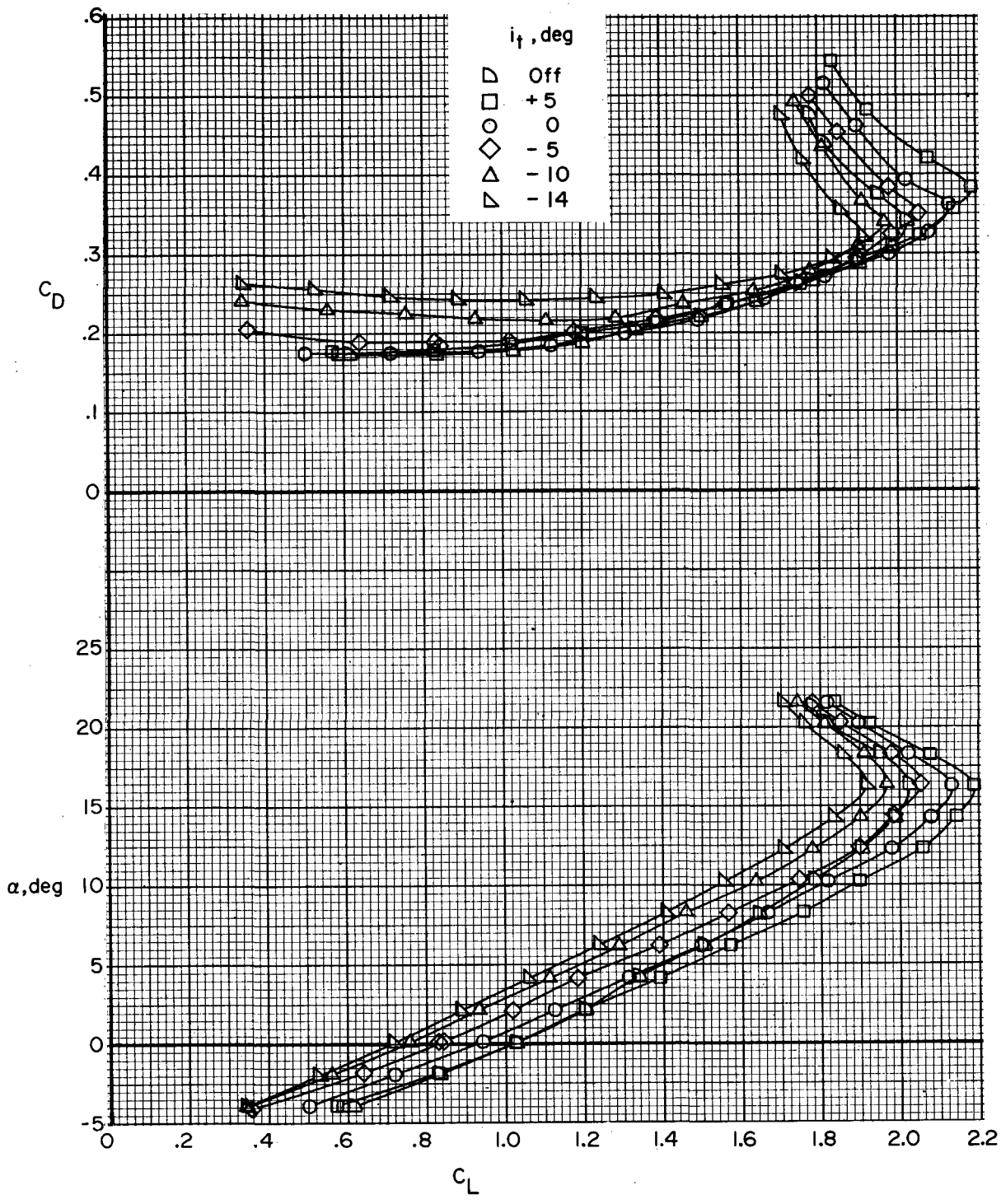

(a) Lift and drag coefficients.

Figure 8.- Effect of horizontal-tail incidence on longitudinal aerodynamic characteristics of transport airplane model. Landing flap configuration; landing gear down.

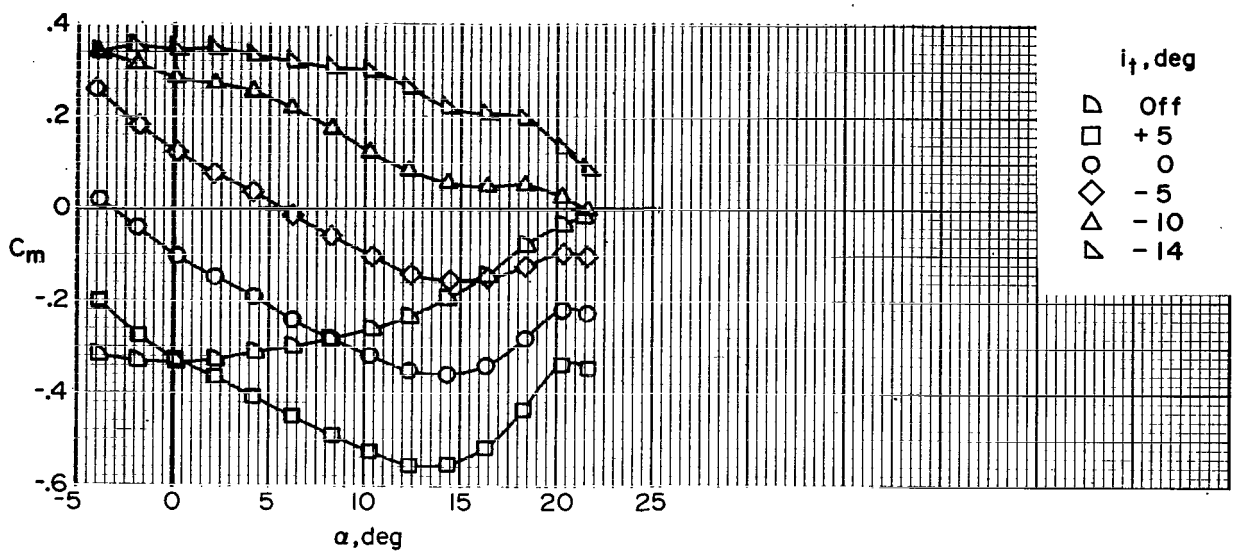

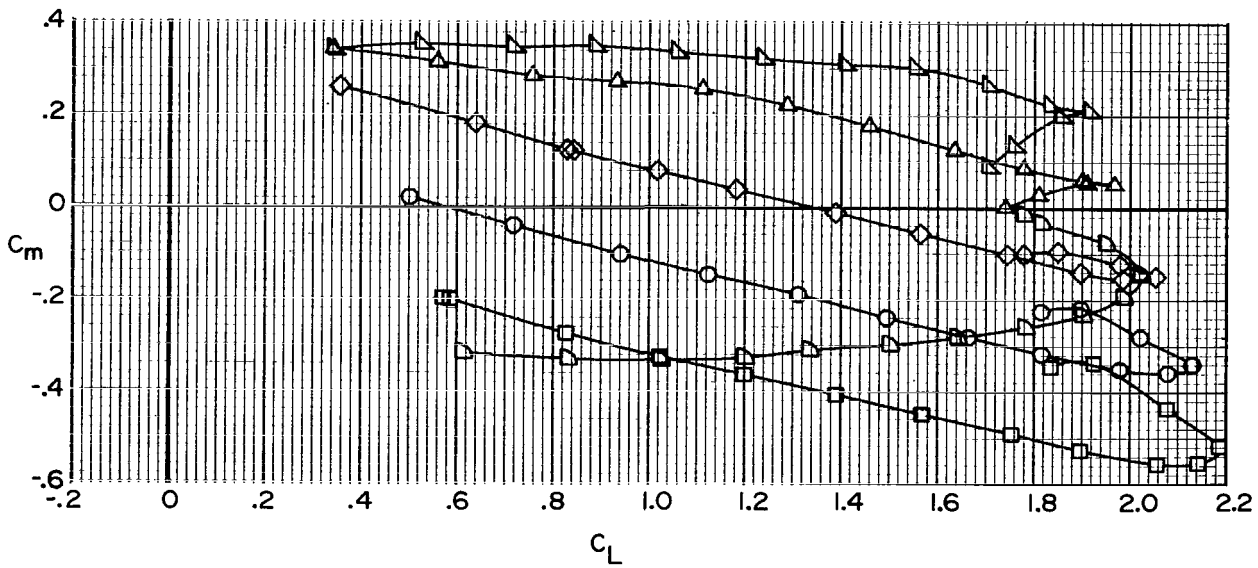

(b) Pitching-moment coefficient.

Figure 8.- Concluded.

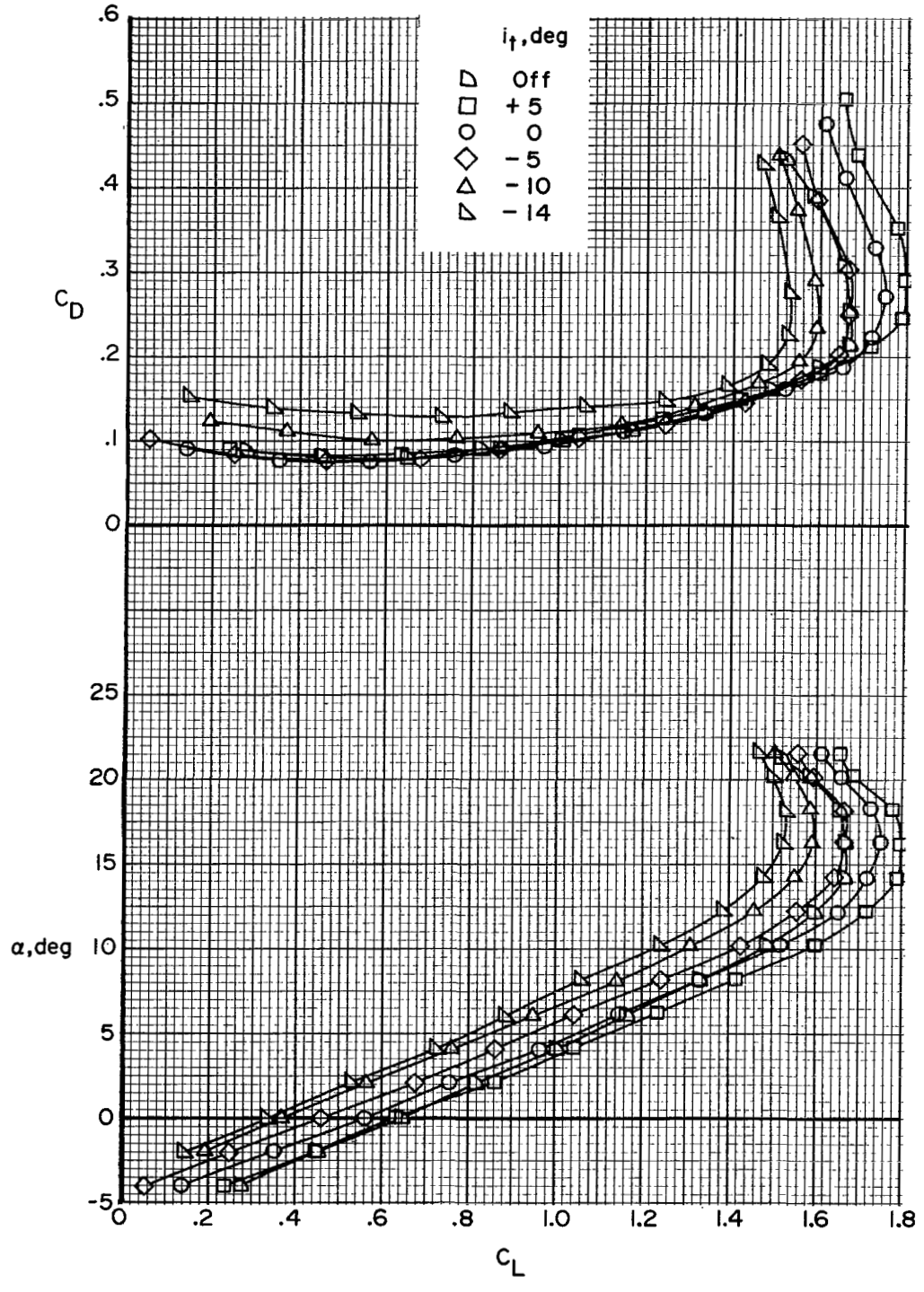

(a) Lift and drag coefficients.

Figure 9.- Effect of horizontal-tail incidence on longitudinal aerodynamic characteristics of transport airplane model. Approach flap configuration; landing gear up.

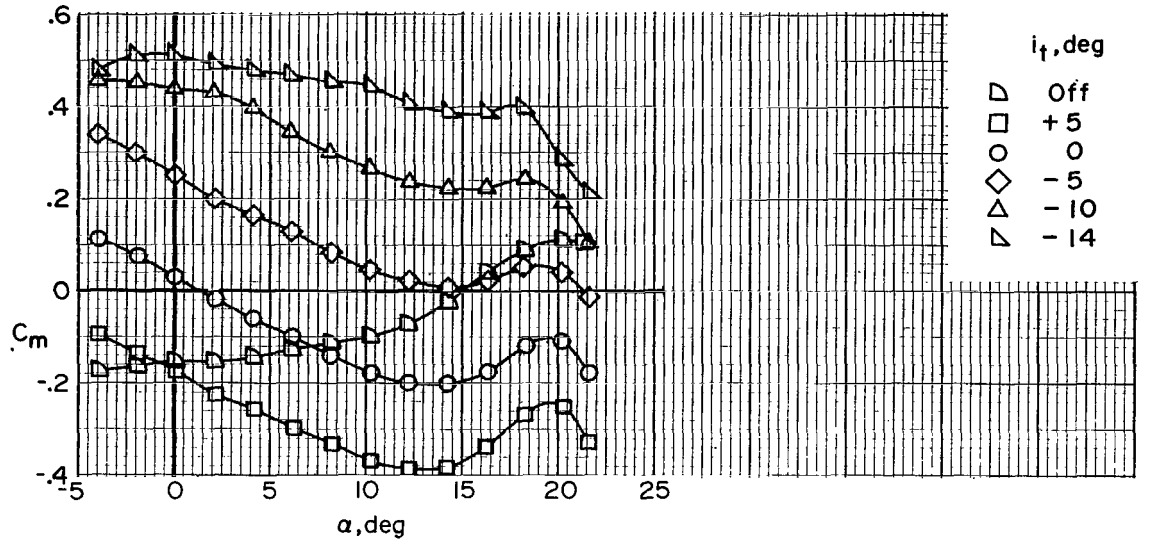

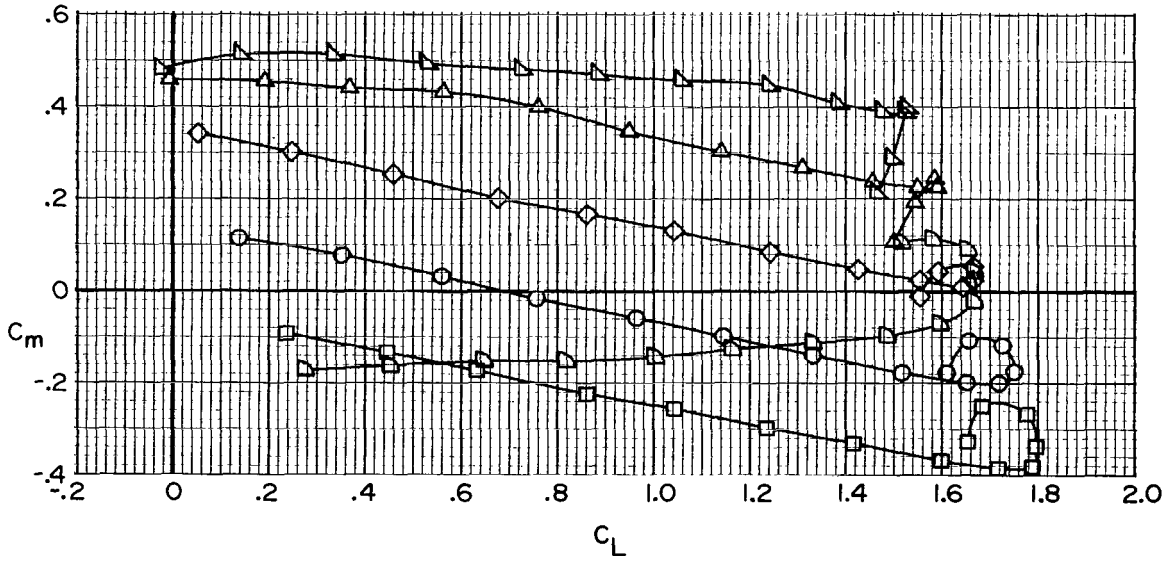

(b) Pitching-moment coefficient.

Figure 9.- Concluded.

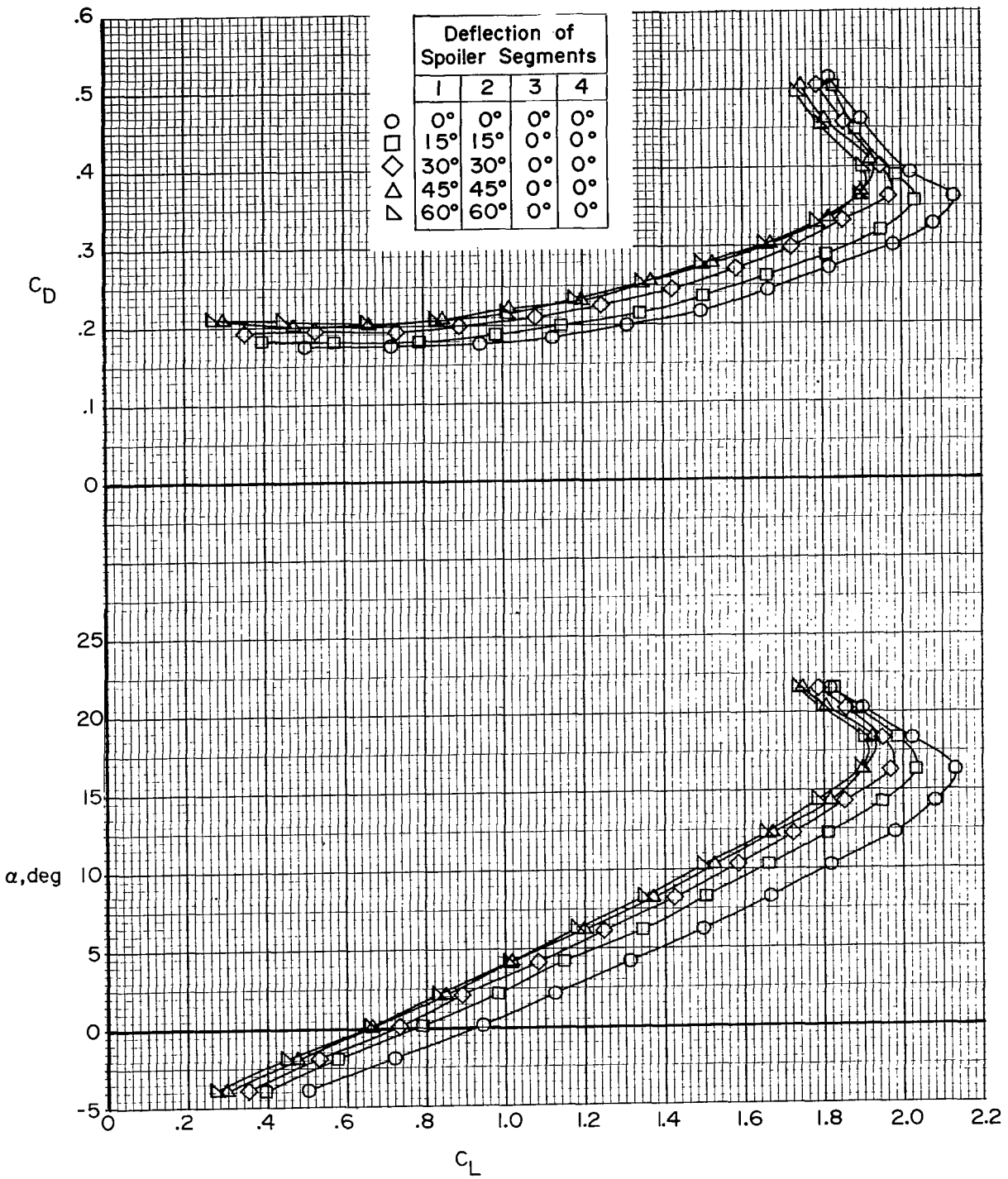

(a) Lift and drag coefficients.

Figure 10.- Effect of deflection angle of flight-spoiler segments 1 and 2 on longitudinal aerodynamic characteristics of transport airplane model. $i_t = 0^o$; landing flap configuration; landing gear down.

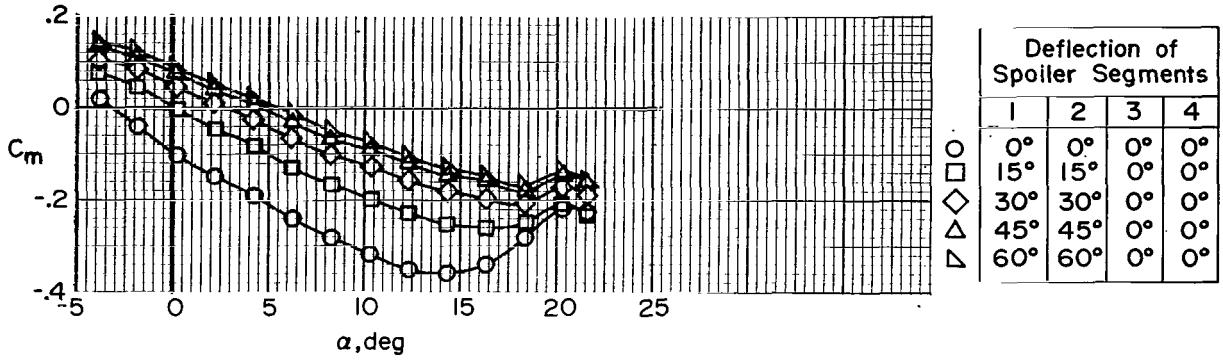

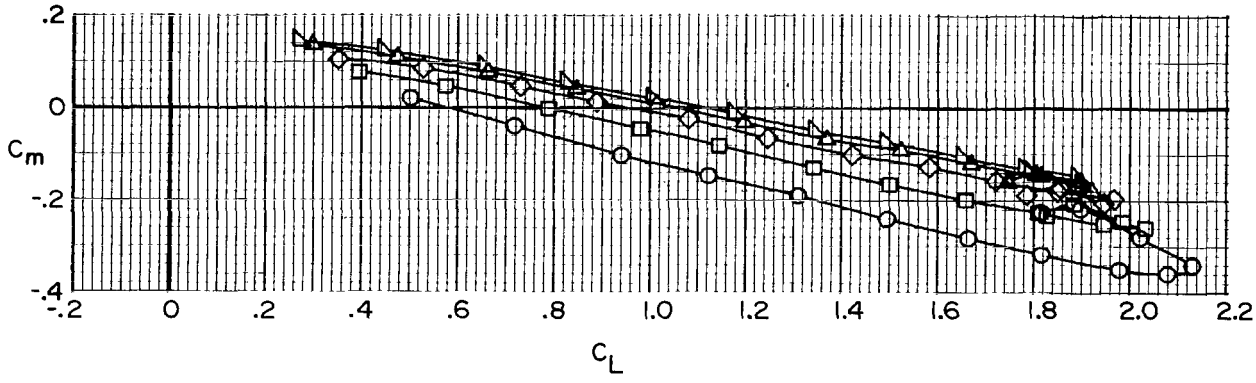

(b) Pitching-moment coefficient.

Figure 10.- Concluded.

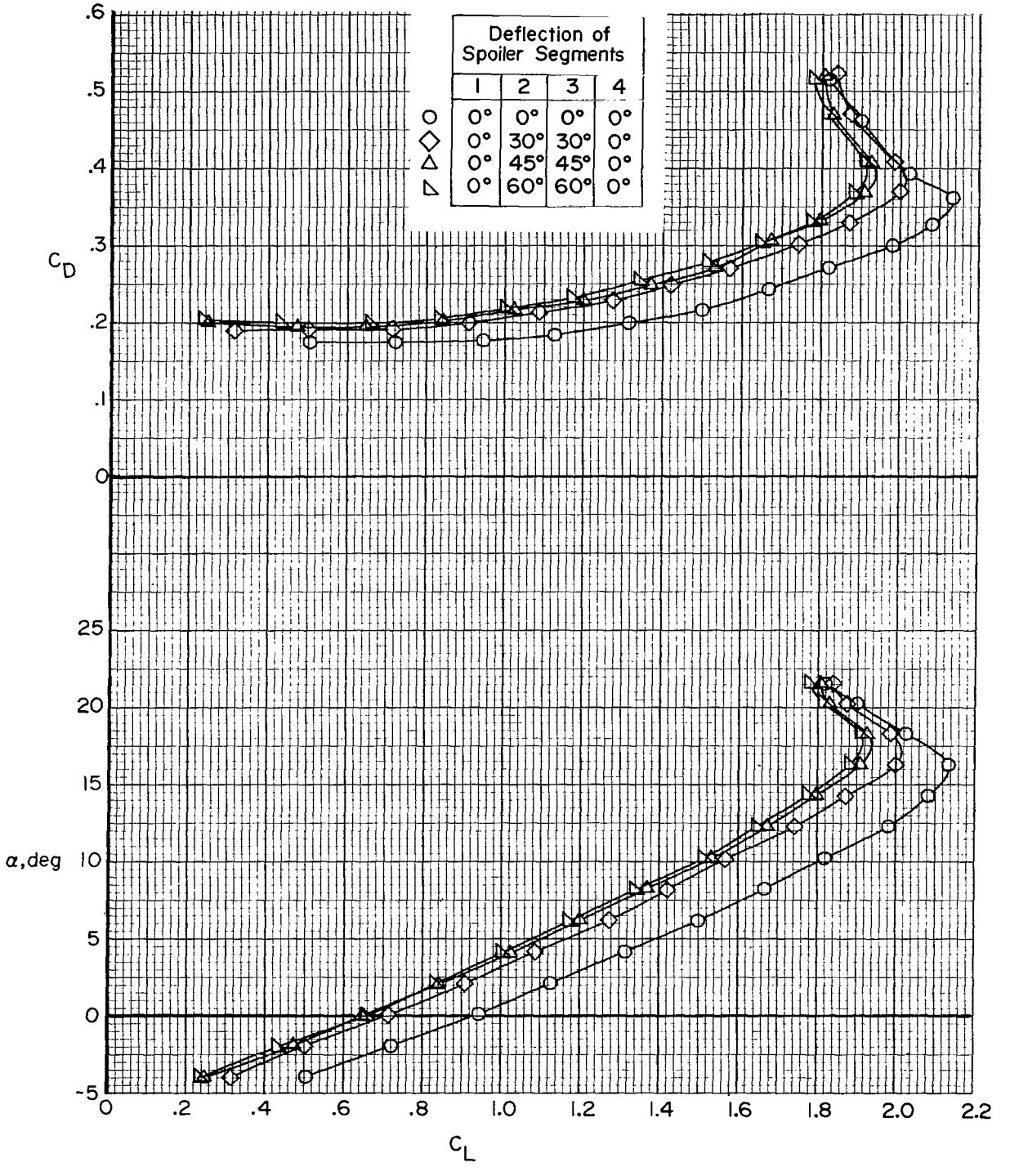

(a) Lift and drag coefficients.

Figure 11.- Effect of deflection angle of flight-spoiler segments 2 and 3 on longitudinal aerodynamic characteristics of transport airplane model. $i_t = 0^o$; landing flap configuration; landing gear down; spoiler segment simulated with wedges.

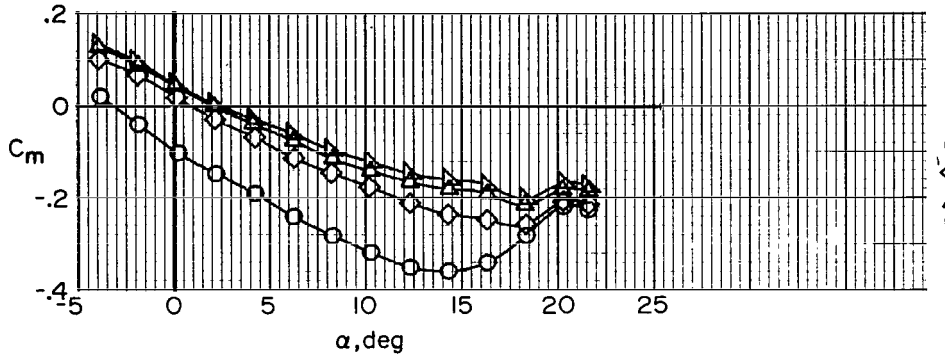

	Deflection of Spoiler Segments			
	1	2	3	4
○	0°	0°	0°	0°
◇	0°	30°	30°	0°
△	0°	45°	45°	0°
▷	0°	60°	60°	0°

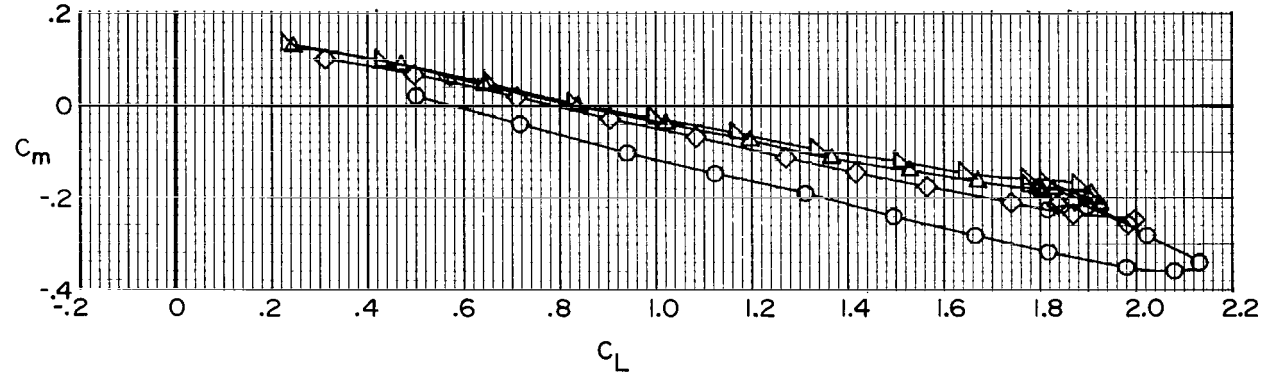

(b) Pitching-moment coefficient.

Figure 11.- Concluded.

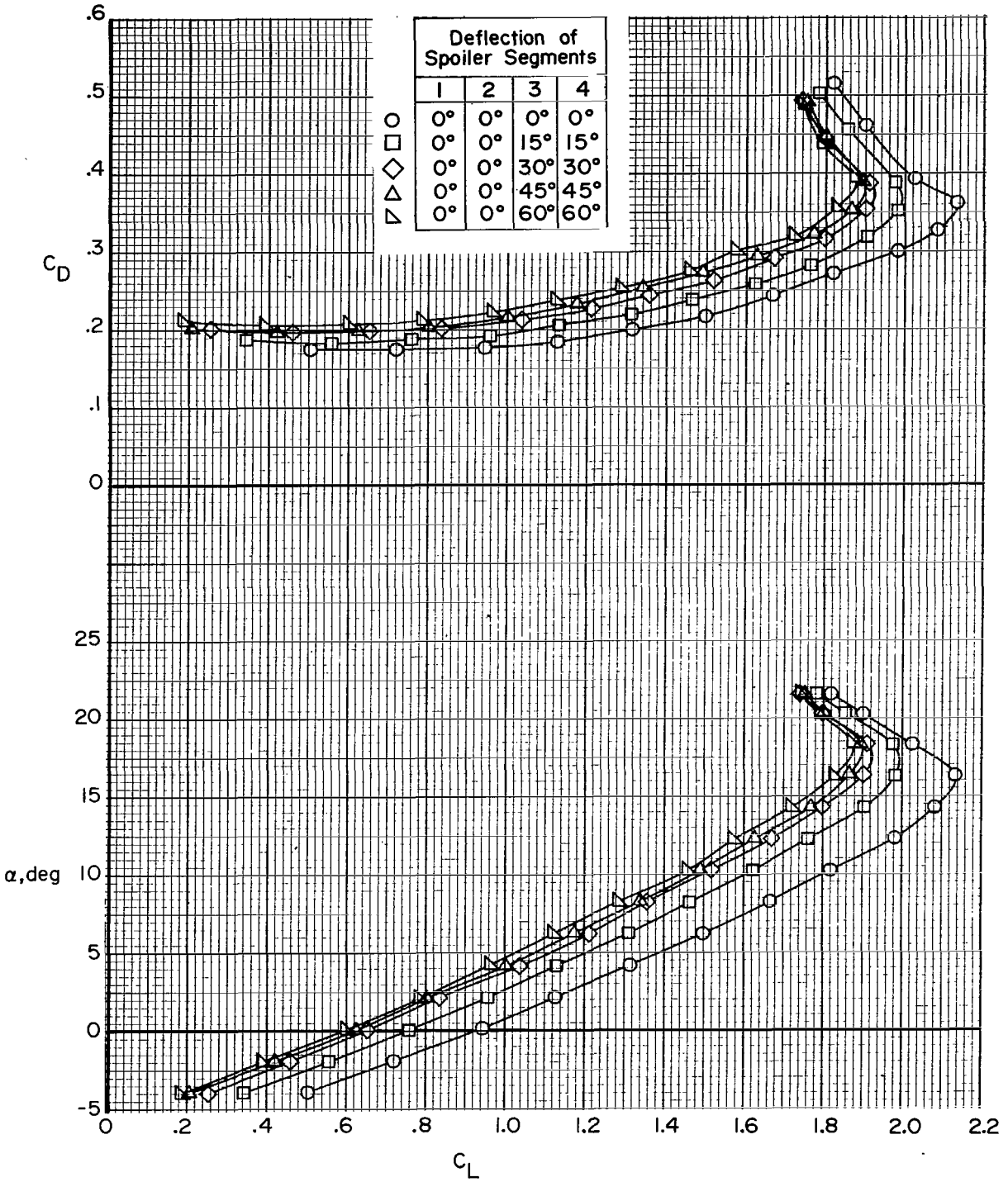

(a) Lift and drag coefficients.

Figure 12.- Effect of deflection angle of flight-spoiler segments 3 and 4 on longitudinal aerodynamic characteristics of transport airplane model. $i_t = 0^o$; landing flap configuration; landing gear down.

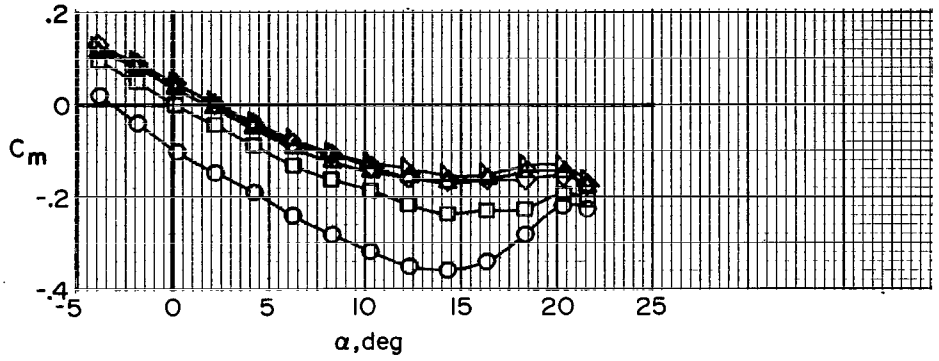

	Deflection of Spoiler Segments			
	1	2	3	4
○	0°	0°	0°	0°
□	0°	0°	15°	15°
◇	0°	0°	30°	30°
△	0°	0°	45°	45°
◁	0°	0°	60°	60°

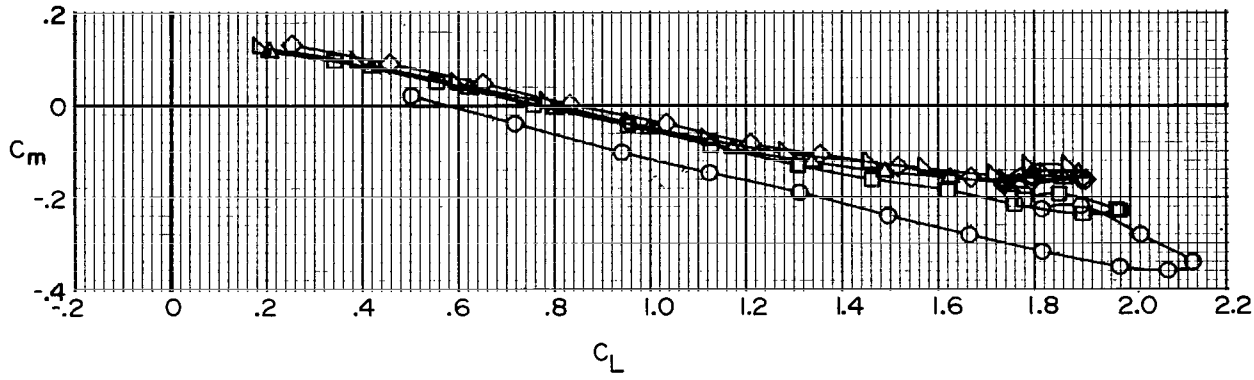

(b) Pitching-moment coefficient.

Figure 12.- Concluded.

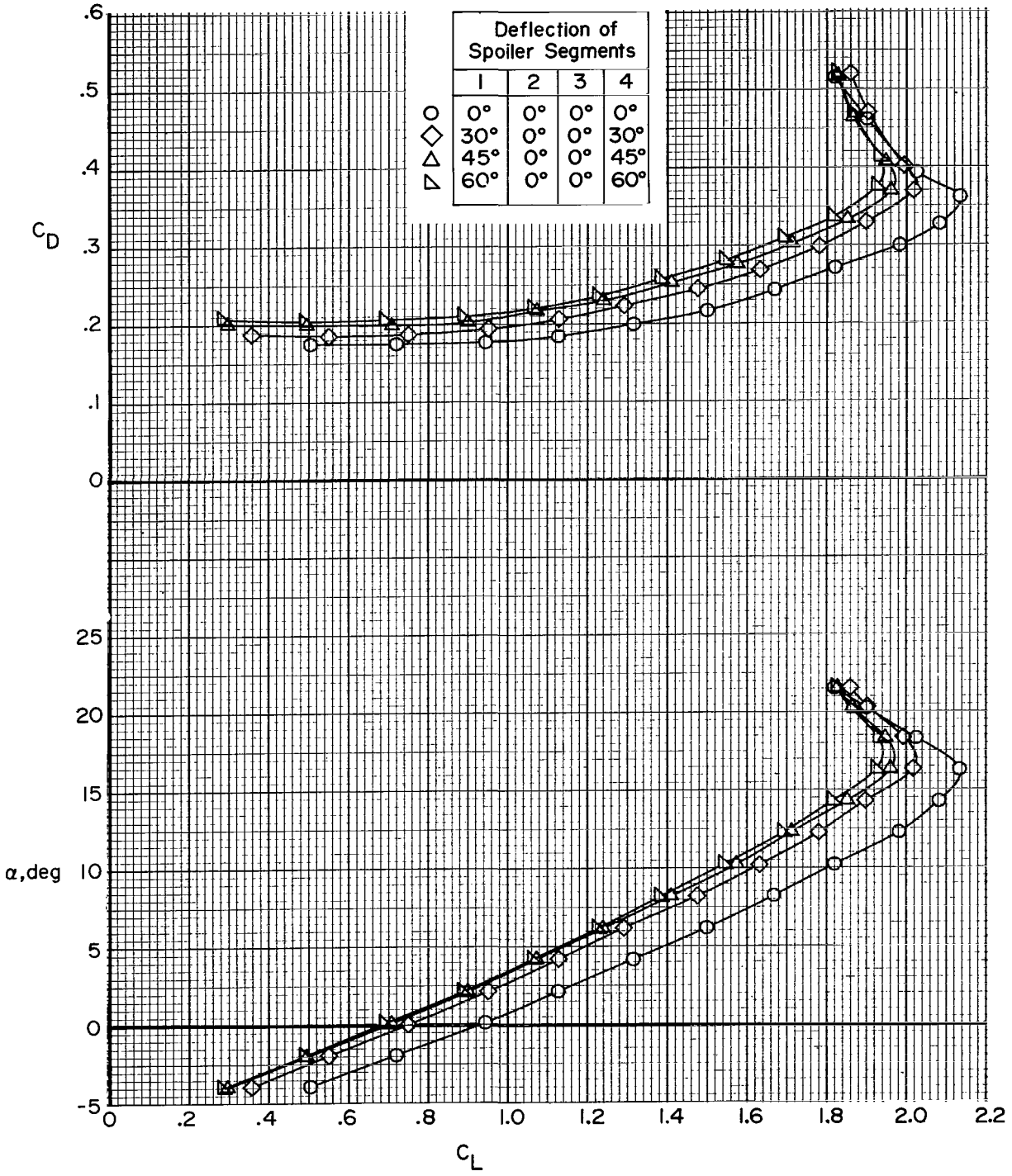

(a) Lift and drag coefficients.

Figure 13.- Effect of deflection angle of flight-spoiler segments 1 and 4 on longitudinal aerodynamic characteristics of transport airplane model. $i_t = 0^o$; landing flap configuration; landing gear down; spoiler segments simulated with wedges.

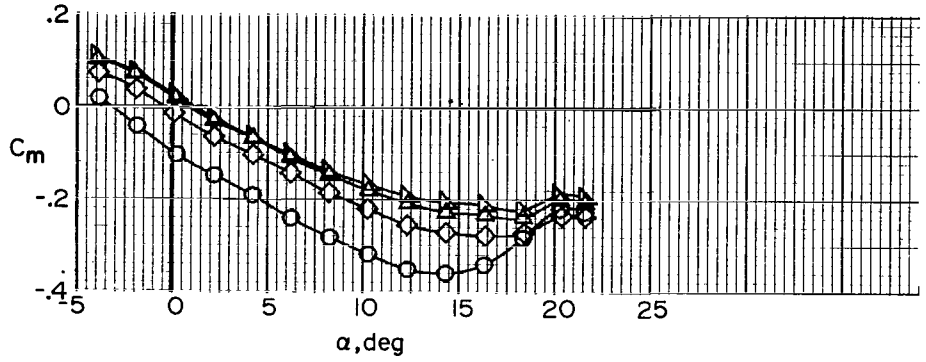

	Deflection of Spoiler Segments			
	1	2	3	4
○	0°	0°	0°	0°
◇	30°	0°	0°	30°
△	45°	0°	0°	45°
▷	60°	0°	0°	60°

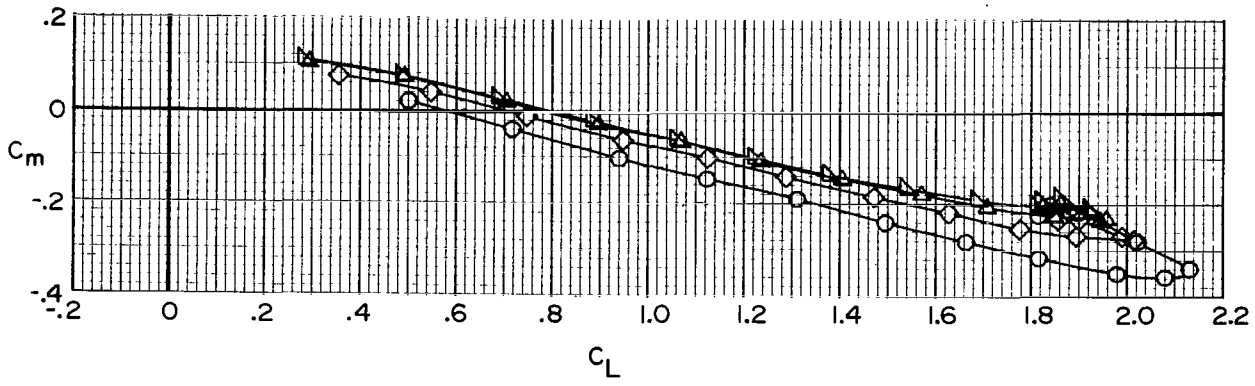

(b) Pitching-moment coefficient.

Figure 13.- Concluded.

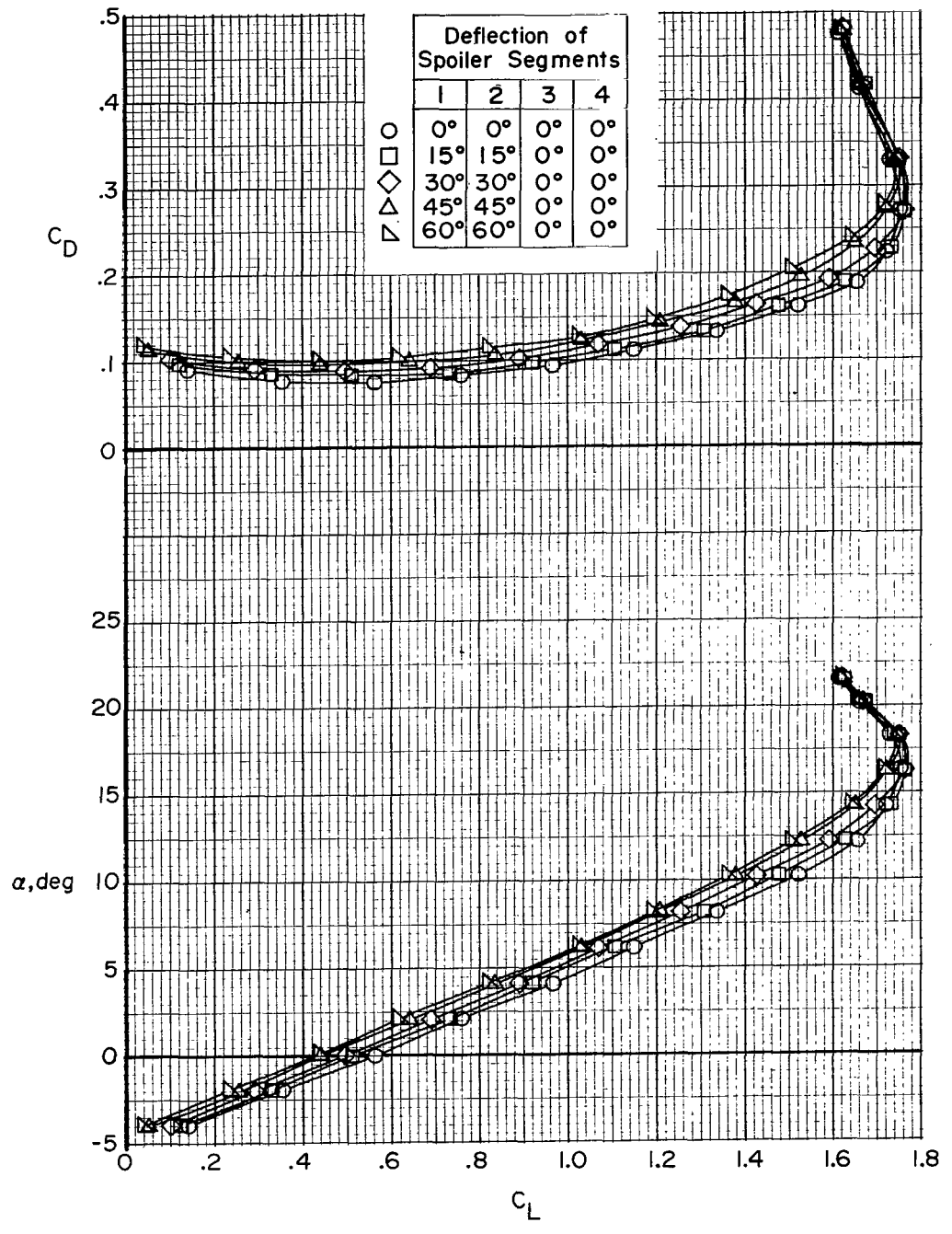

(a) Lift and drag coefficients.

Figure 14.- Effect of deflection angle of flight-spoiler segments 1 and 2 on longitudinal aerodynamic characteristics of transport airplane model. i_t = 0°; approach flap configuration; landing gear up.

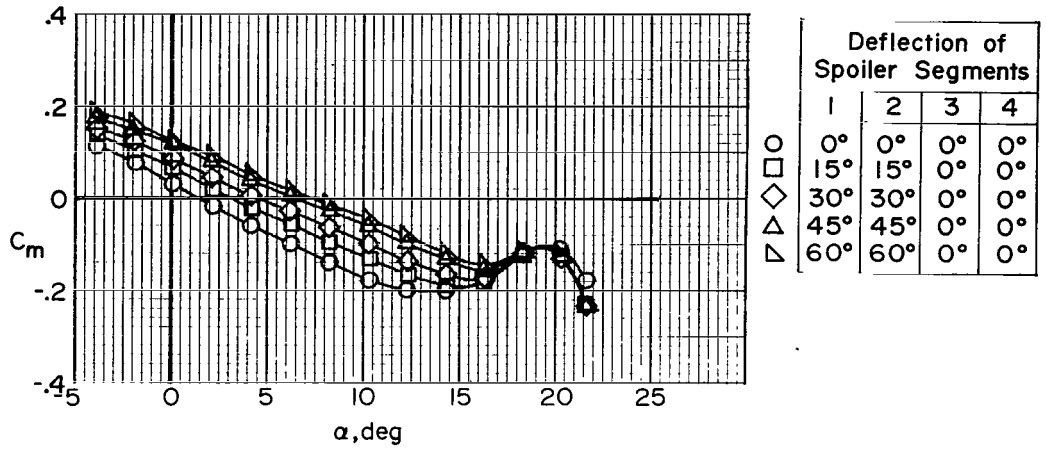

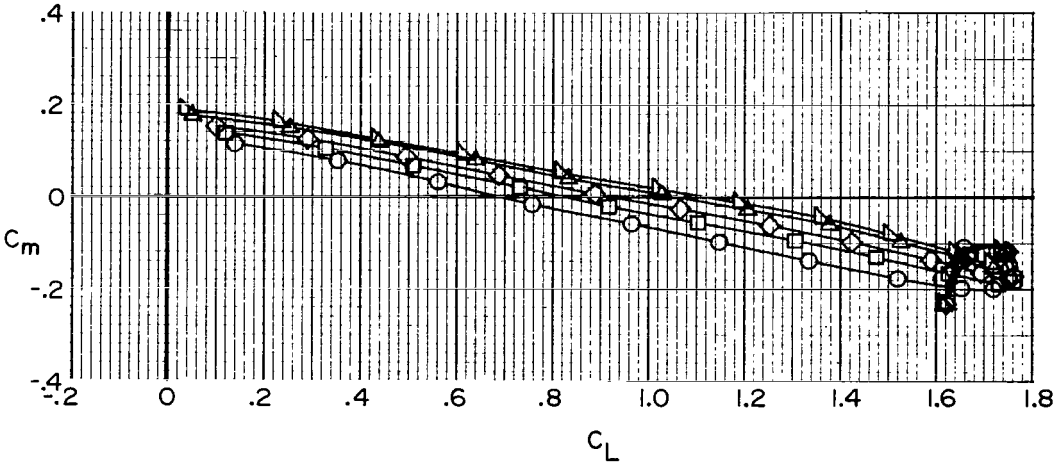

(b) Pitching-moment coefficient.

Figure 14.- Concluded.

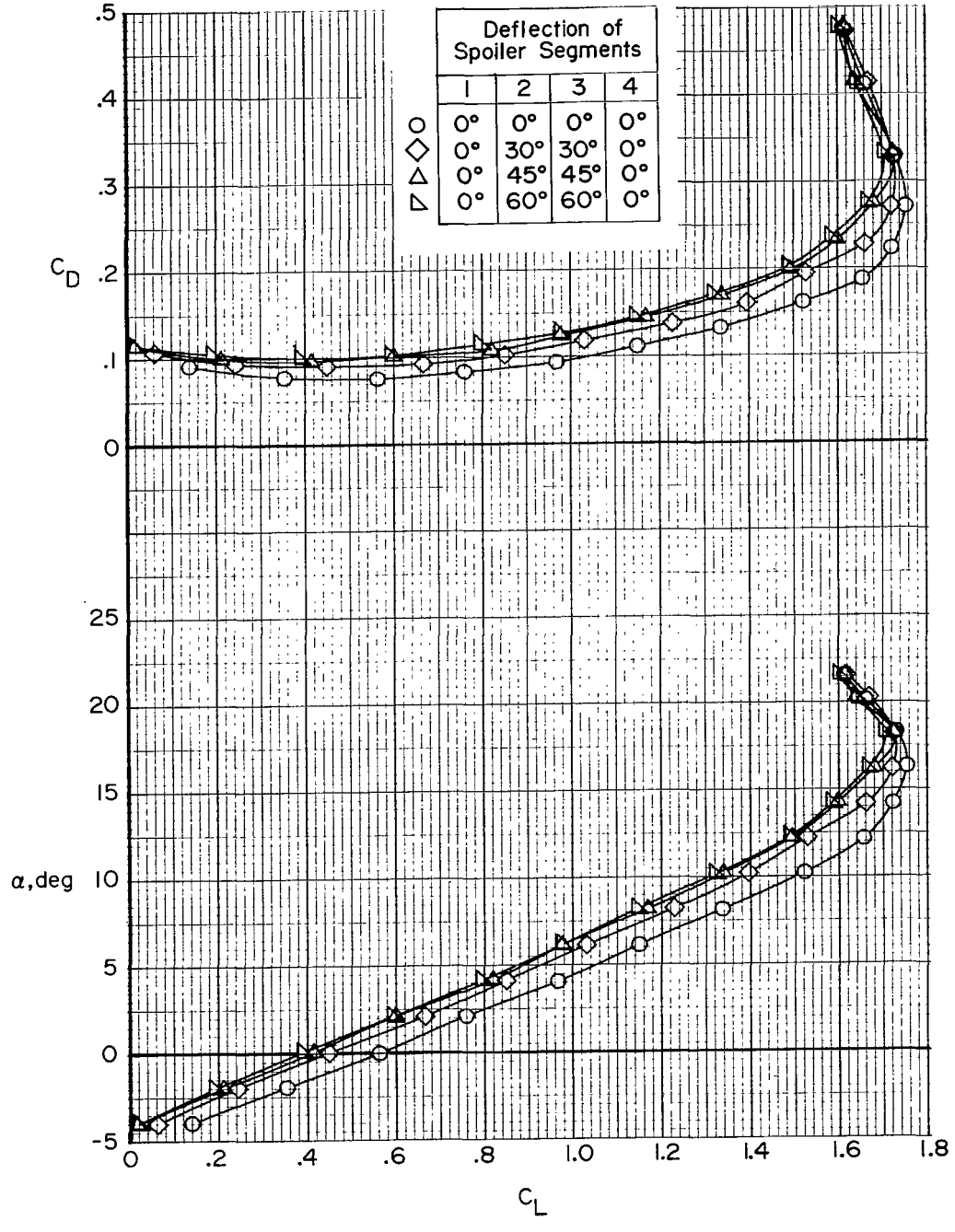

(a) Lift and drag coefficients.

Figure 15.- Effect of deflection angle of flight-spoiler segments 2 and 3 on longitudinal aerodynamic characteristics of transport airplane model. i_t = 0°; approach flap configuration; landing gear up; spoiler segments simulated with wedges.

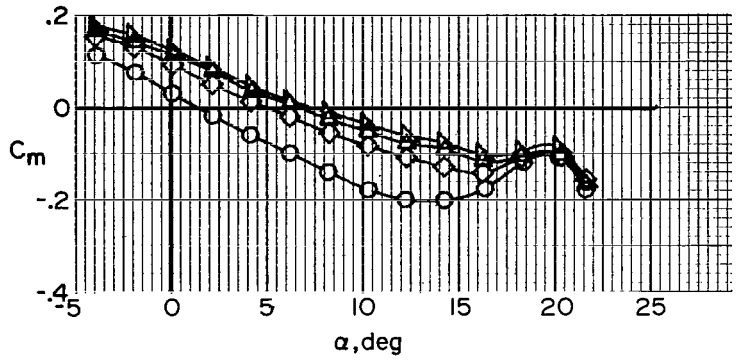

	Deflection of Spoiler Segments			
	1	2	3	4
○	0°	0°	0°	0°
◇	0°	30°	30°	0°
△	0°	45°	45°	0°
▷	0°	60°	60°	0°

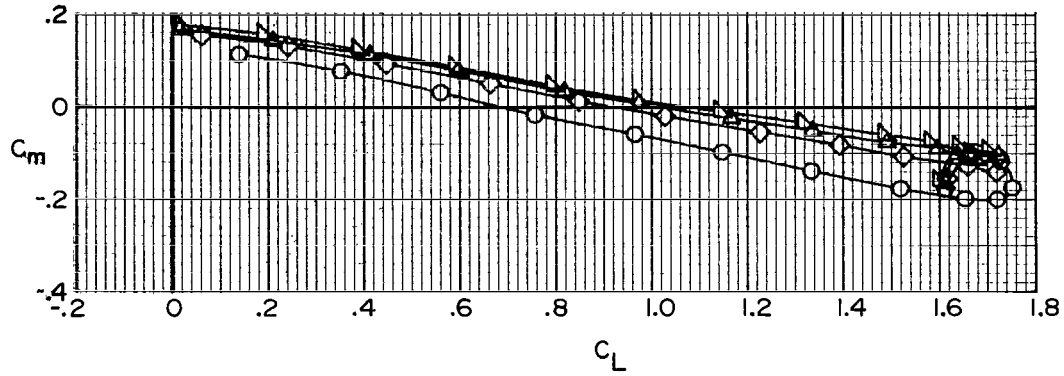

(b) Pitching-moment coefficient.

Figure 15.- Concluded.

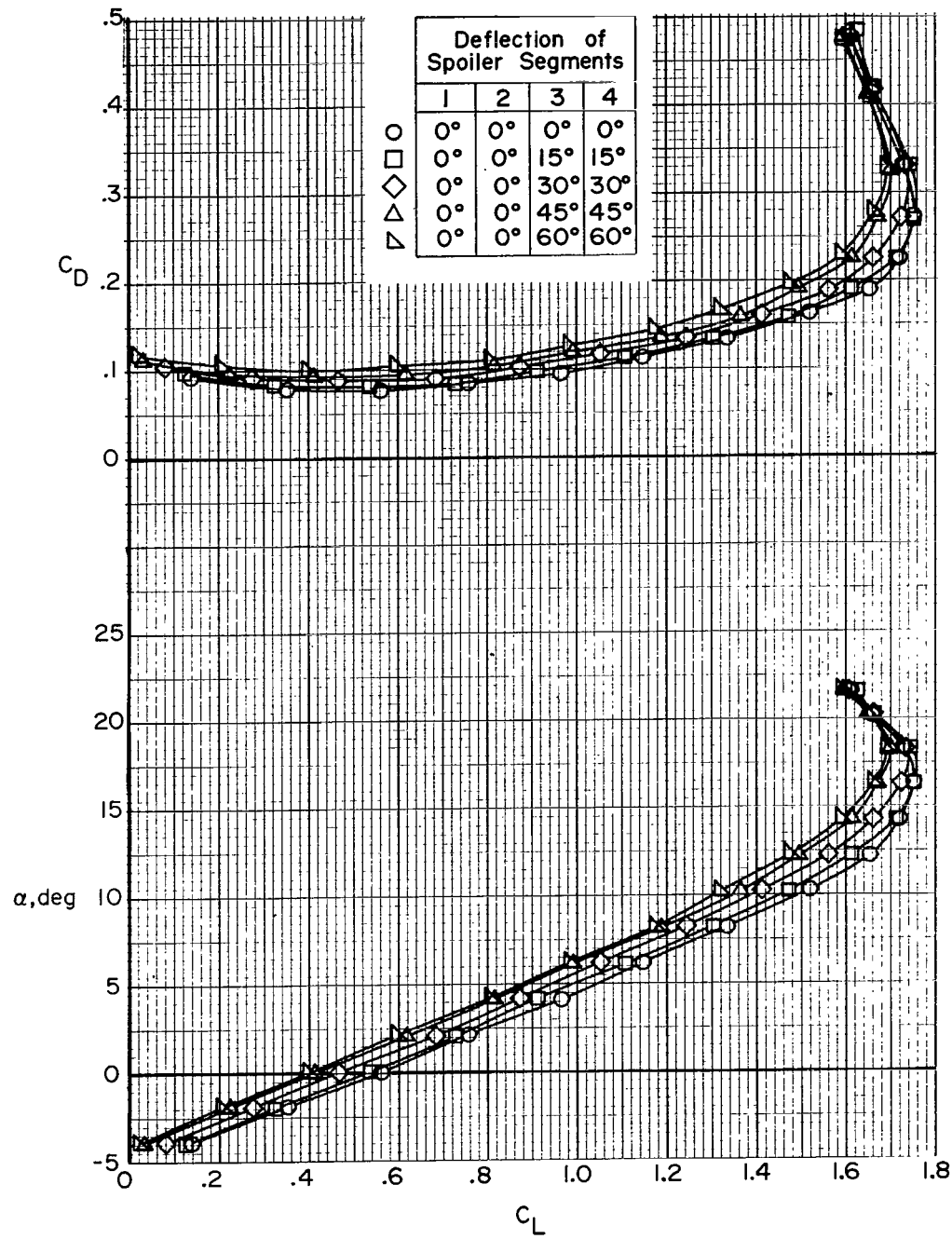

(a) Lift and drag coefficients.

Figure 16.- Effect of deflection angle of flight-spoiler segments 3 and 4 on longitudinal aerodynamic characteristics of transport airplane model. $i_t = 0^o$; approach flap configuration; landing gear up.

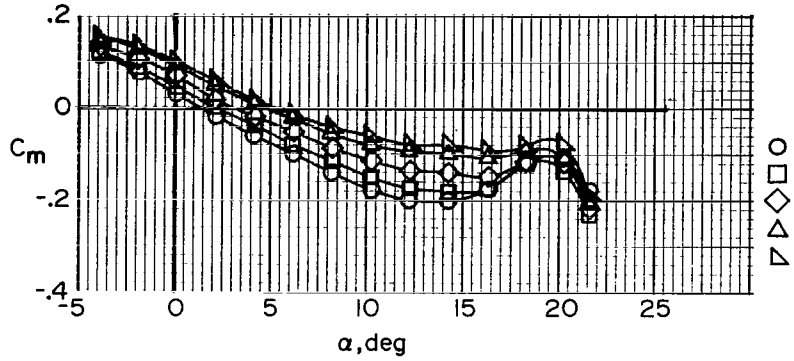

	Deflection of Spoiler Segments			
	1	2	3	4
○	0°	0°	0°	0°
□	0°	0°	15°	15°
◇	0°	0°	30°	30°
△	0°	0°	45°	45°
▷	0°	0°	60°	60°

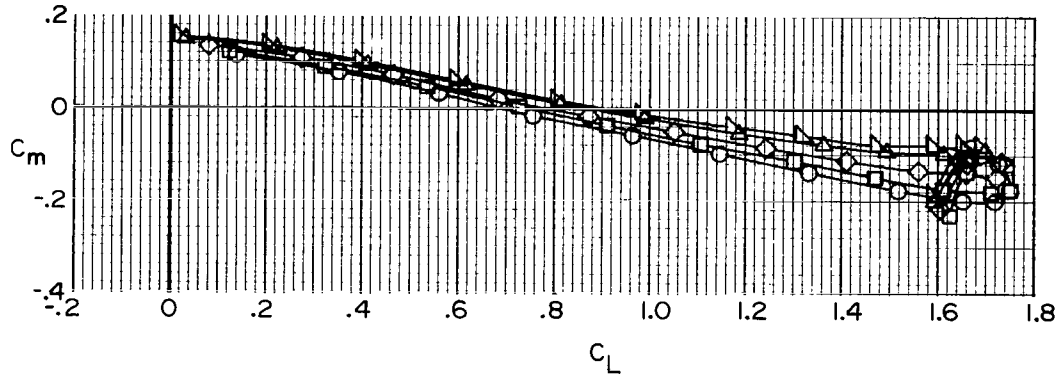

(b) Pitching-moment coefficient.

Figure 16.- Concluded.

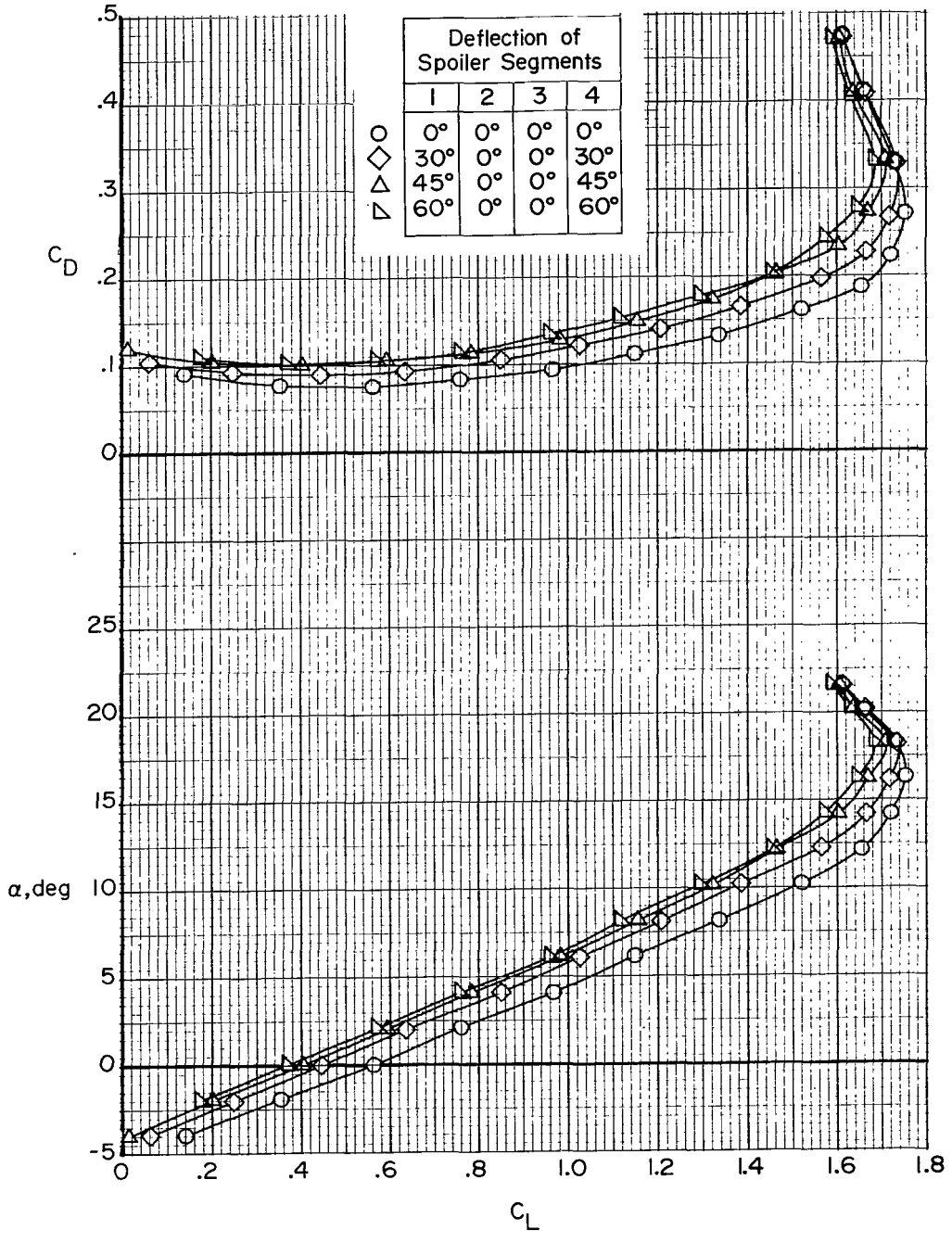

(a) Lift and drag coefficients.

Figure 17.- Effect of deflection angle of flight-spoiler segments 1 and 4 on longitudinal aerodynamic characteristics of transport airplane model. $i_t = 0^o$; approach flap configuration; landing gear up; spoiler segments simulated with wedges.

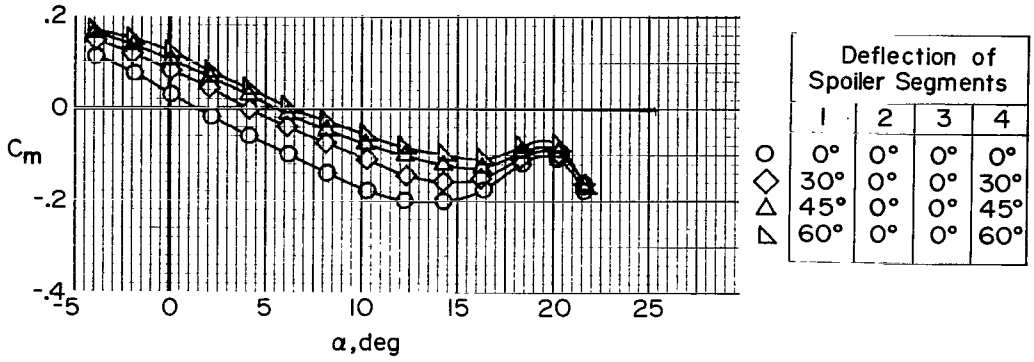

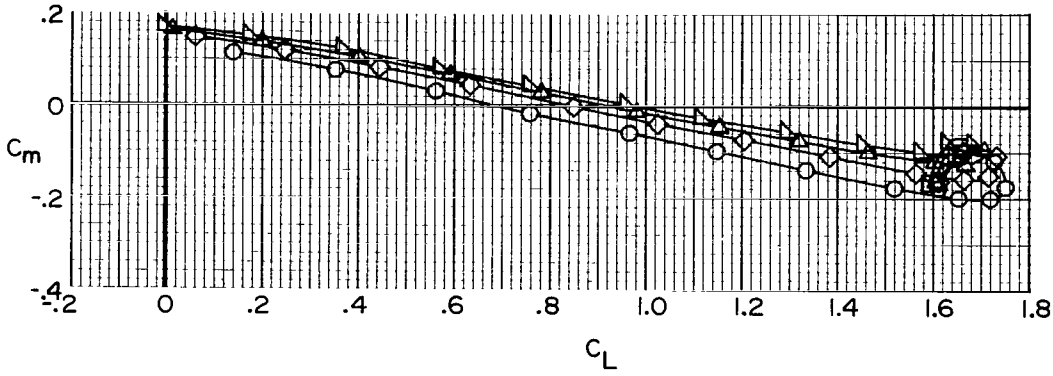

(b) Pitching-moment coefficient.

Figure 17.- Concluded.

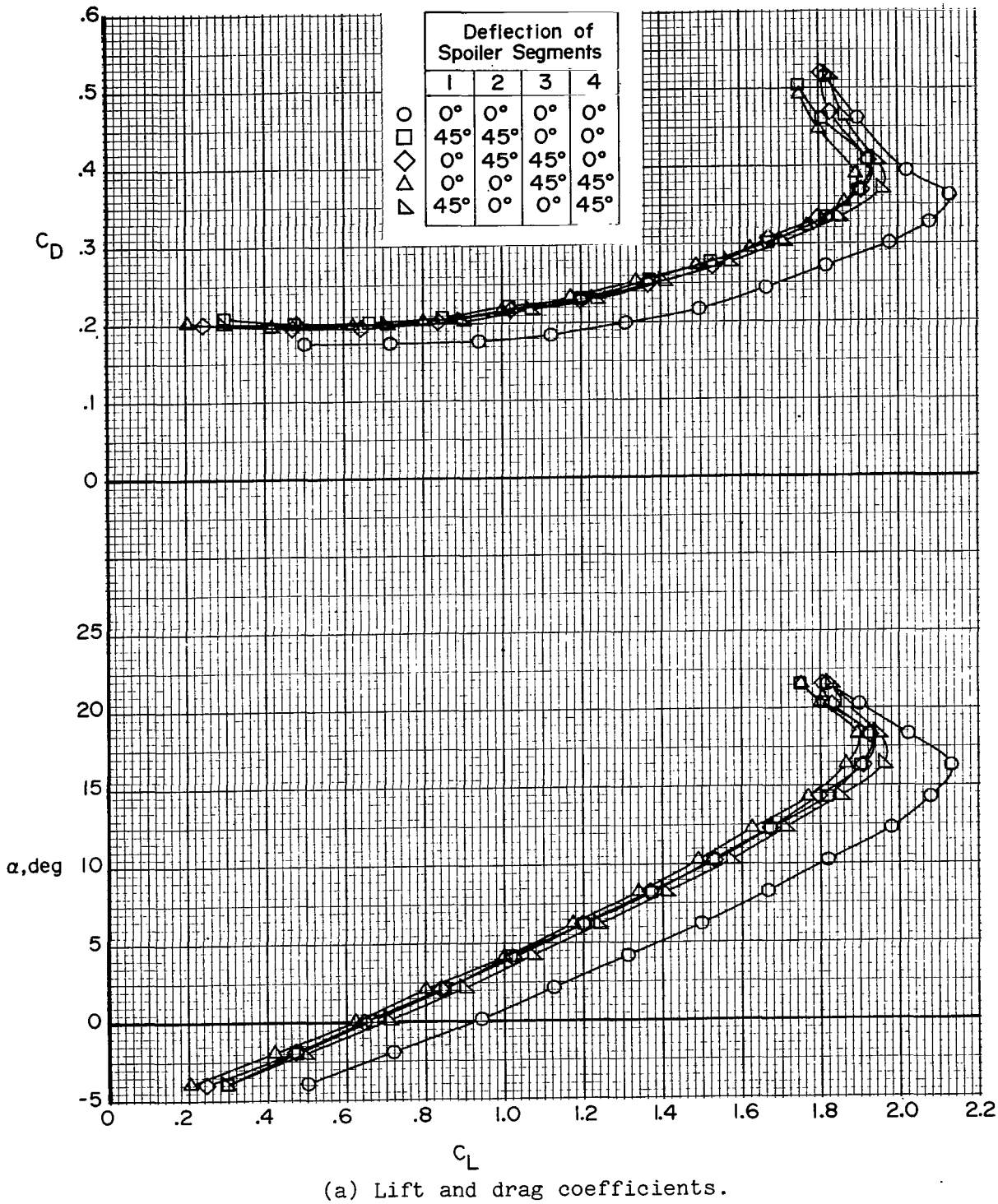

(a) Lift and drag coefficients.

Figure 18.- Effect of flight-spoiler segments 1 and 2, 2 and 3, 3 and 4, and 1 and 4 deflected 45° on longitudinal aerodynamic characteristics of transport airplane model. $i_t = 0°$; landing flap configuration; landing gear down; flight-spoiler segment combinations of 2 and 3, and 1 and 4 simulated with wedges.

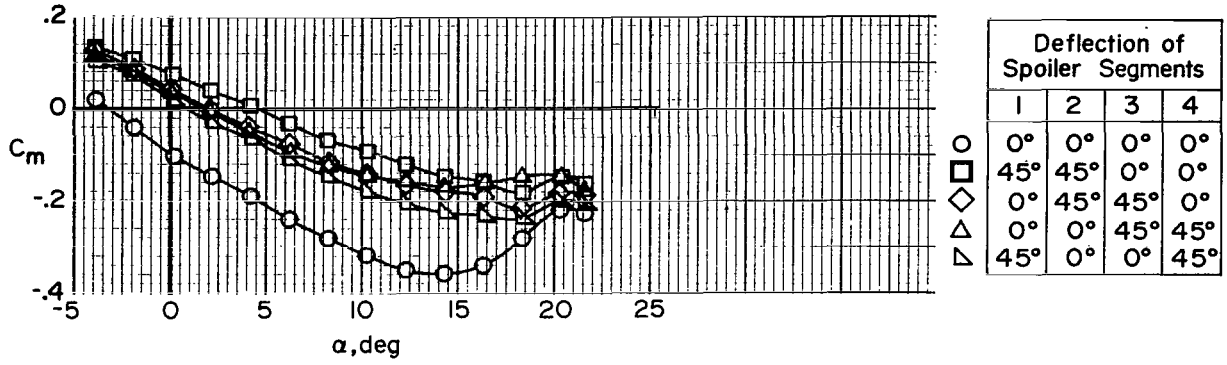

	Deflection of Spoiler Segments			
	1	2	3	4
○	0°	0°	0°	0°
□	45°	45°	0°	0°
◇	0°	45°	45°	0°
△	0°	0°	45°	45°
▷	45°	0°	0°	45°

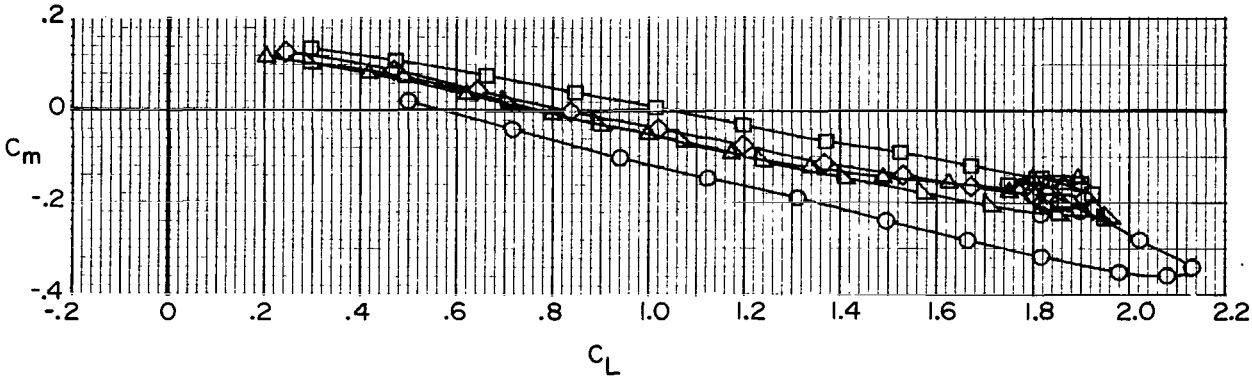

(b) Pitching-moment coefficient.

Figure 18.- Concluded.

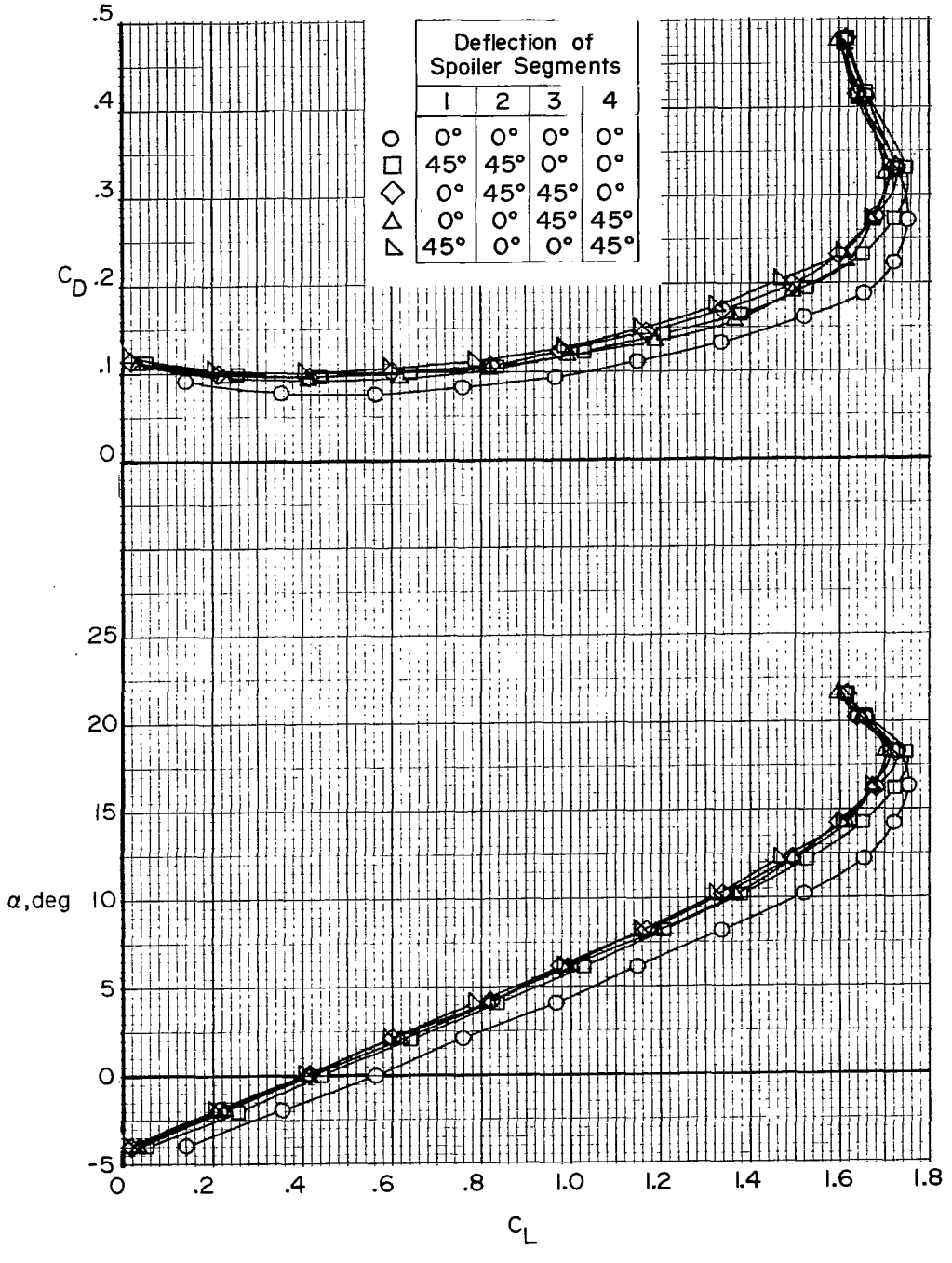

(a) Lift and drag coefficients.

Figure 19.- Effect of flight-spoiler segments 1 and 2, 2 and 3, 3 and 4, and 1 and 4 deflected 45° on longitudinal aerodynamic characteristics of transport airplane model. i_t = 0°; approach flap configuration; landing gear up; flight-spoiler segment combinations of 2 and 3, and 1 and 4 simulated with wedges.

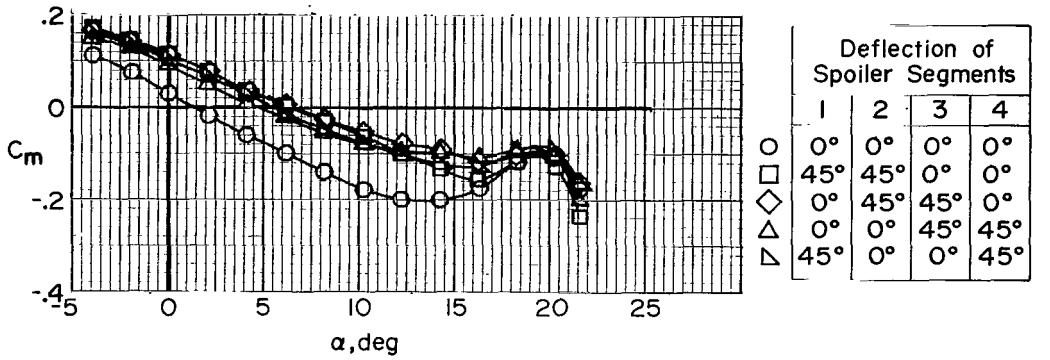

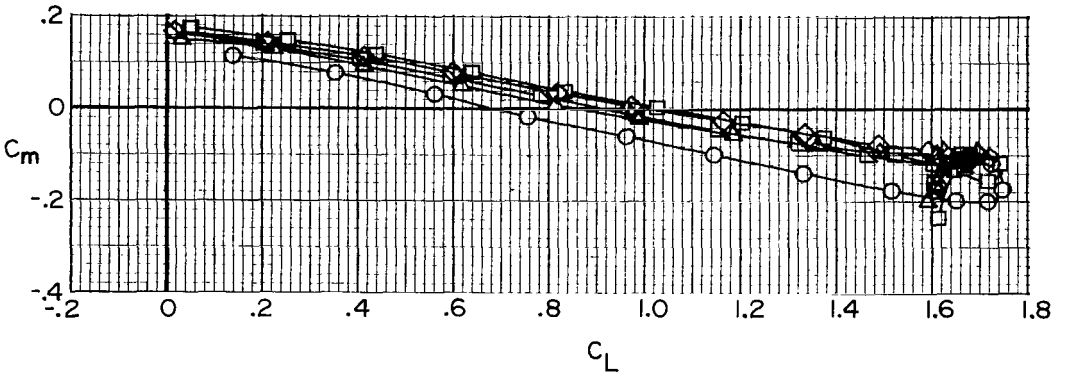

(b) Pitching-moment coefficient.

Figure 19.- Concluded.

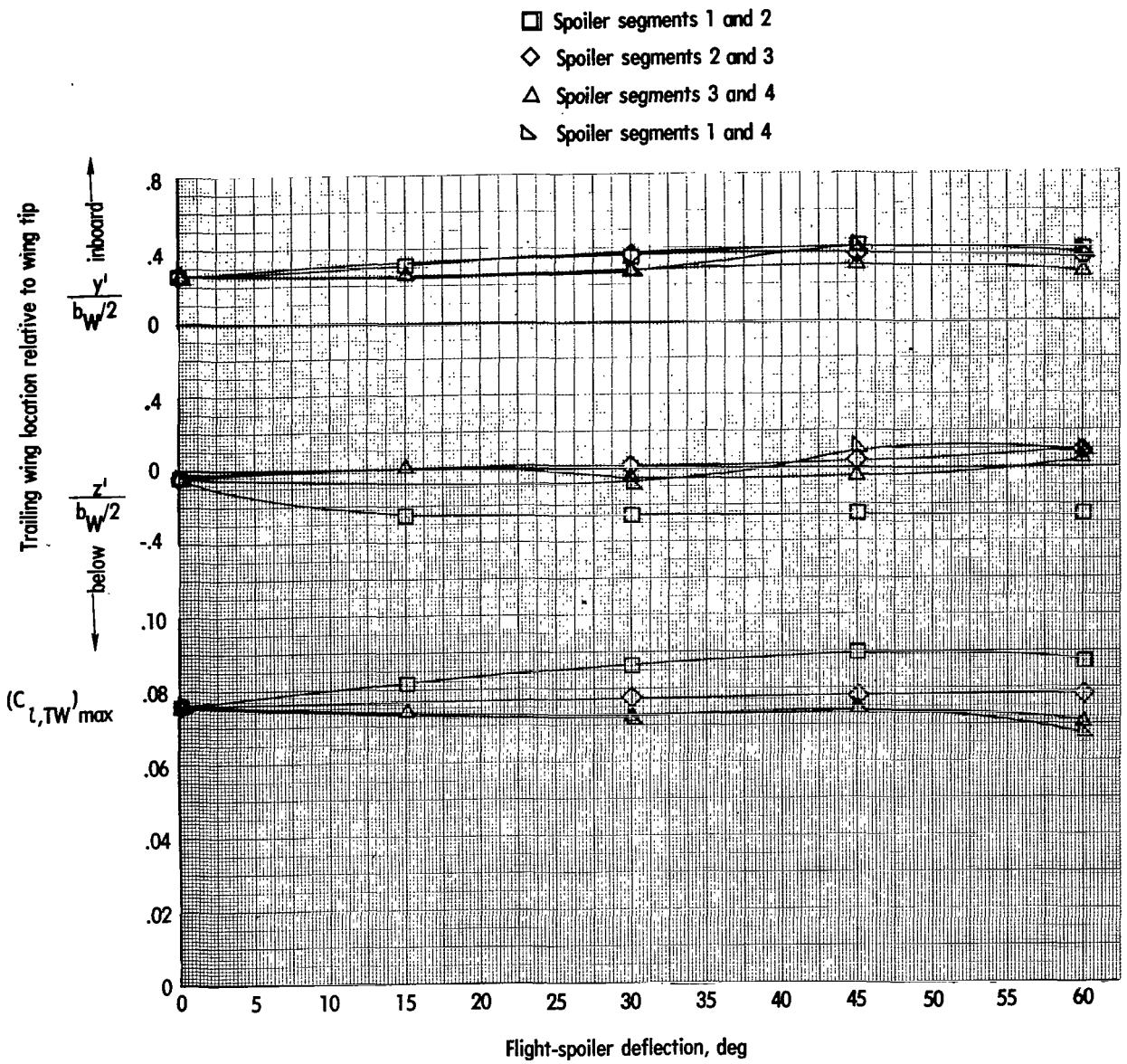

(a) Trailing wing model located 3.7 transport wing spans behind transport airplane model.

Figure 20.- Variation of trailing wing location and rolling-moment coefficient with flight-spoiler deflection for various segments of flight spoilers. $C_{L,trim}$ = 1.2; approach flap configuration; landing gear up; flight-spoiler segment combinations of 2 and 3, and 1 and 4 simulated with wedges.

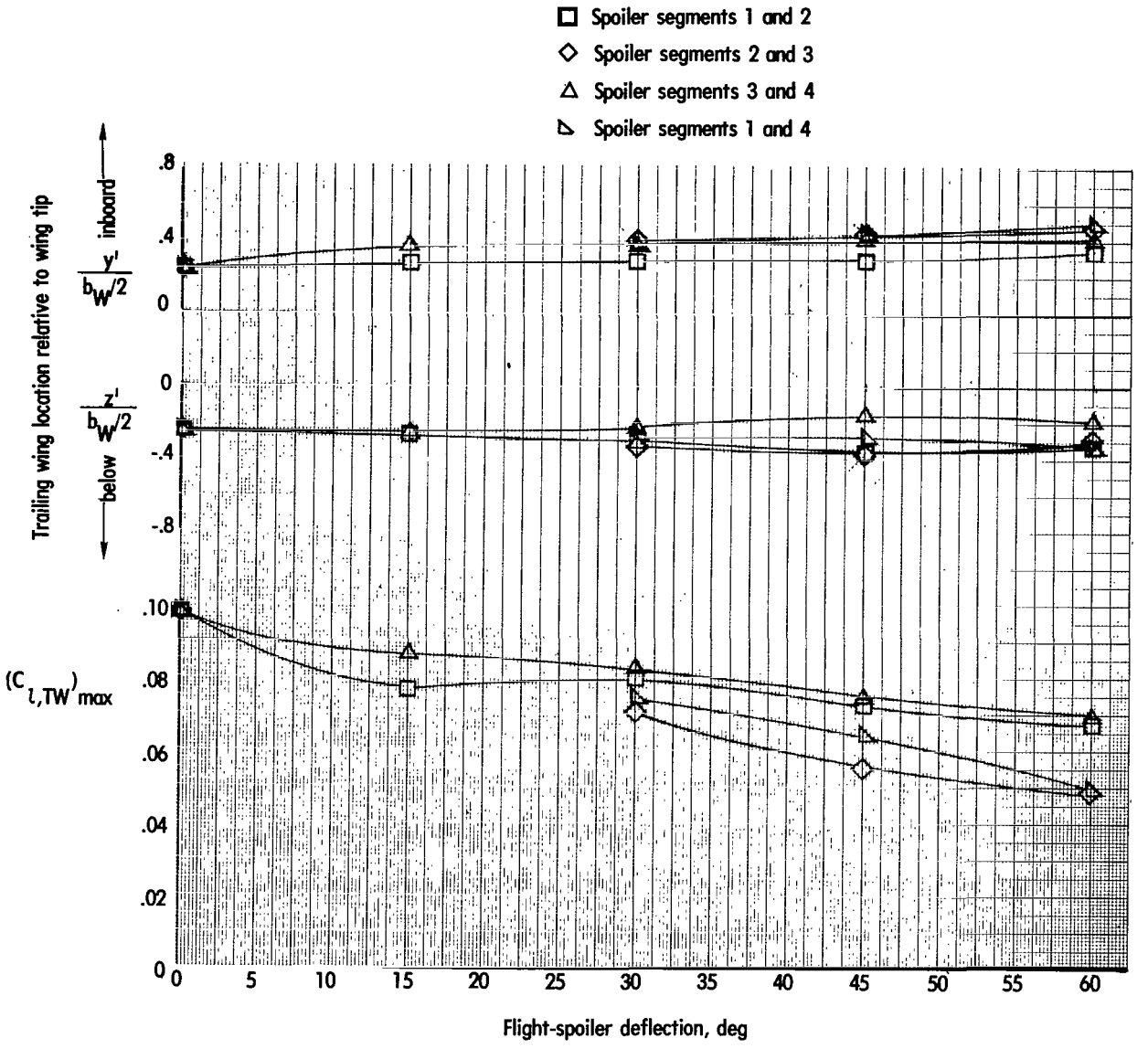

(b) Trailing wing model located 9.2 transport wing spans behind transport airplane model.

Figure 20.- Continued.

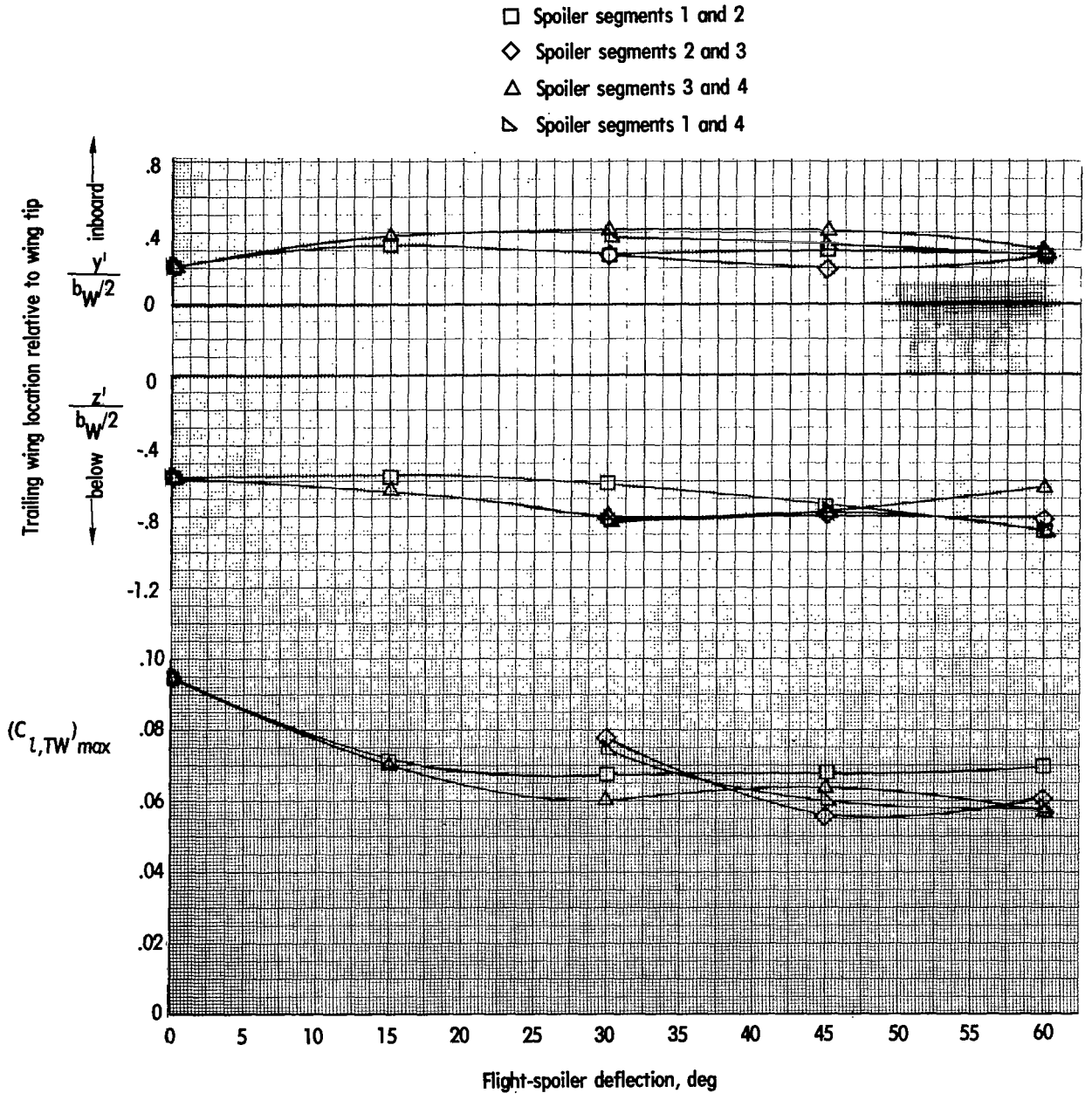

(c) Trailing wing model located 18.4 transport wing spans behind transport airplane model.

Figure 20.- Concluded.

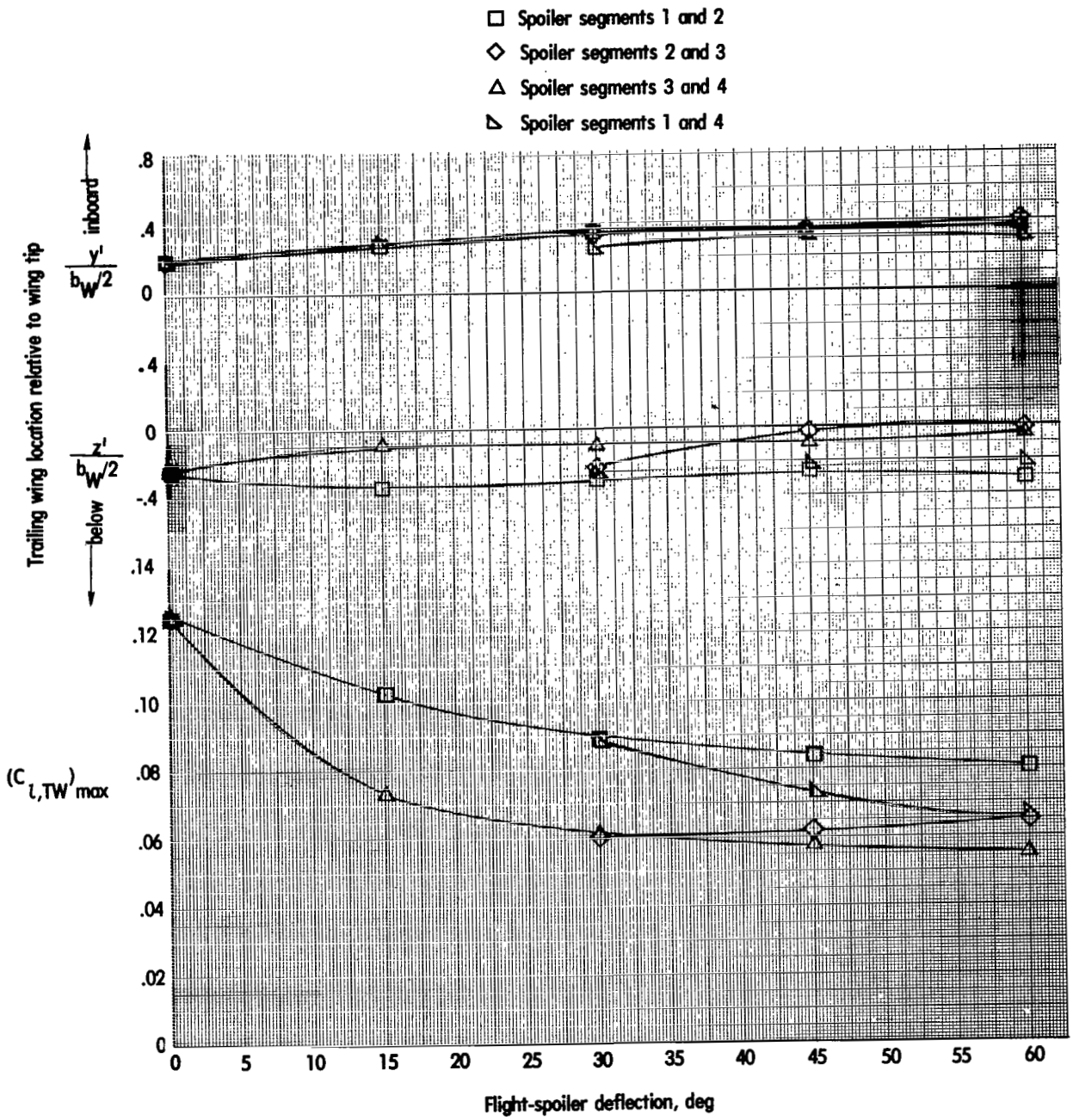

(a) Trailing wing model located 3.7 transport wing spans behind transport airplane model.

Figure 21.- Variation of trailing wing location and rolling-moment coefficient with flight-spoiler deflection for various segments of flight spoilers. $C_{L,trim}$ = 1.2; landing flap configuration; landing gear down; flight-spoiler segment combinations of 2 and 3, and 1 and 4 simulated with wedges.

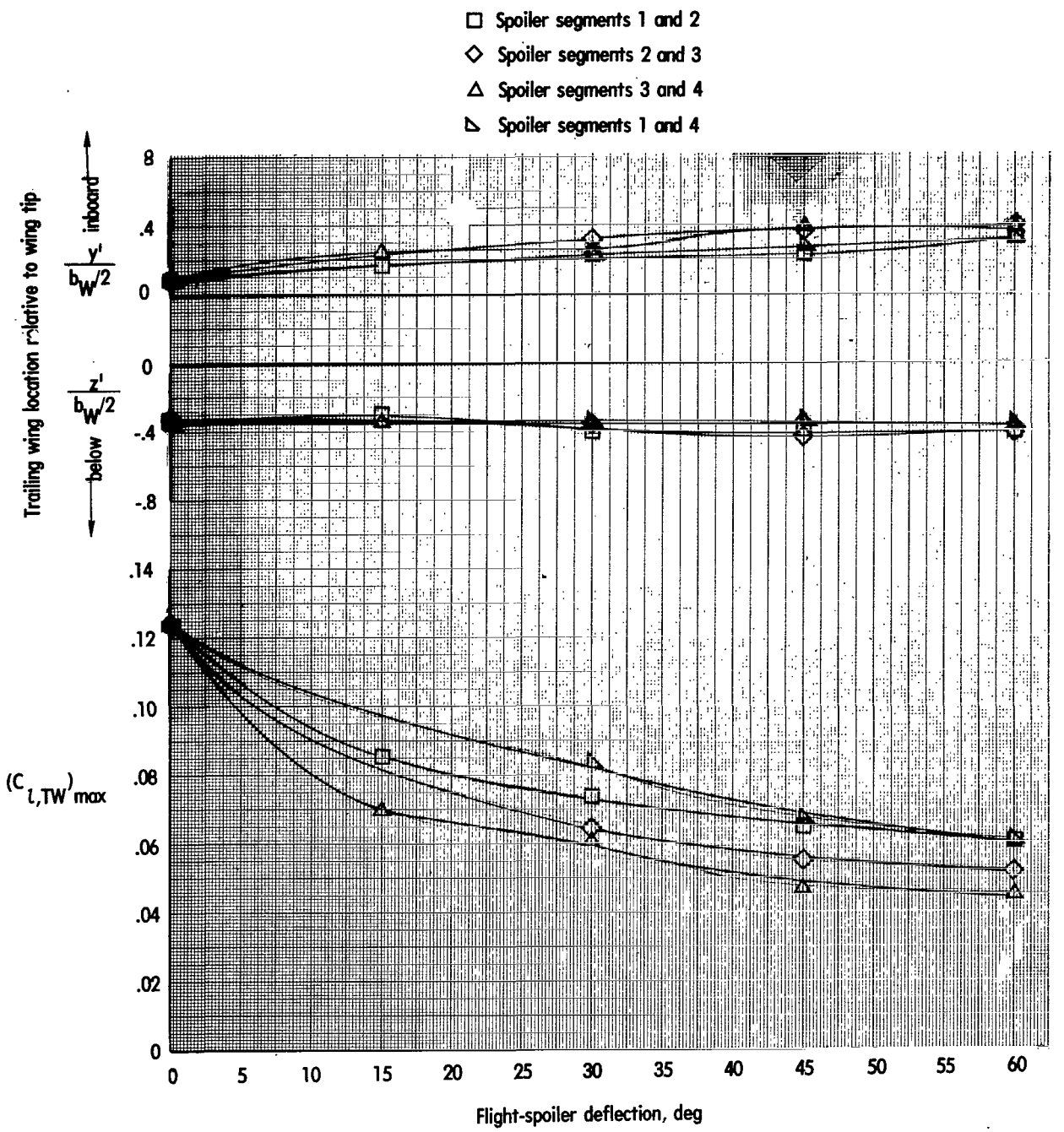

(b) Trailing wing model located 9.2 transport wing spans behind transport airplane model.

Figure 21.- Continued.

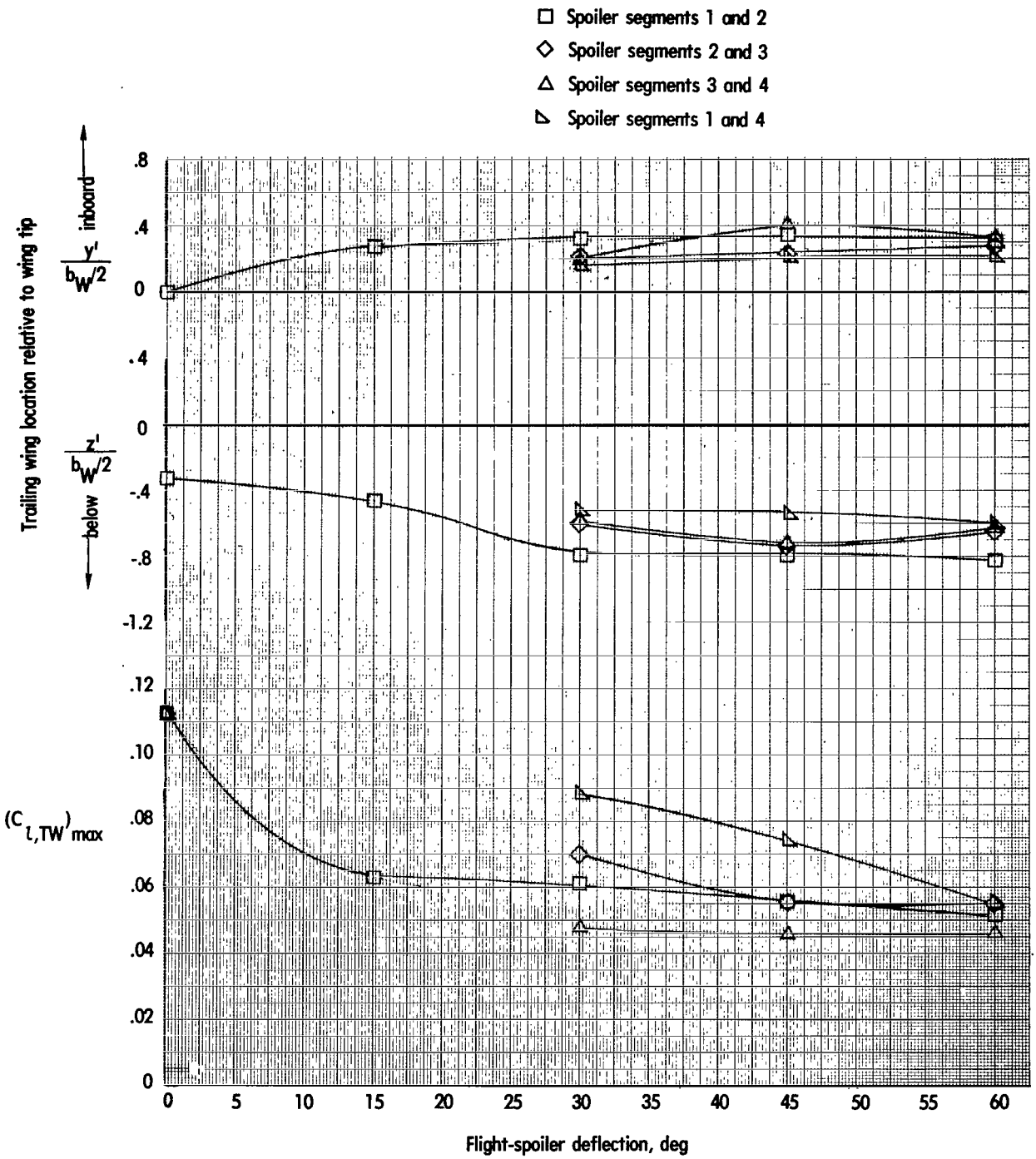

(c) Trailing wing model located 18.4 transport wing spans behind transport airplane model.

Figure 21.- Concluded.

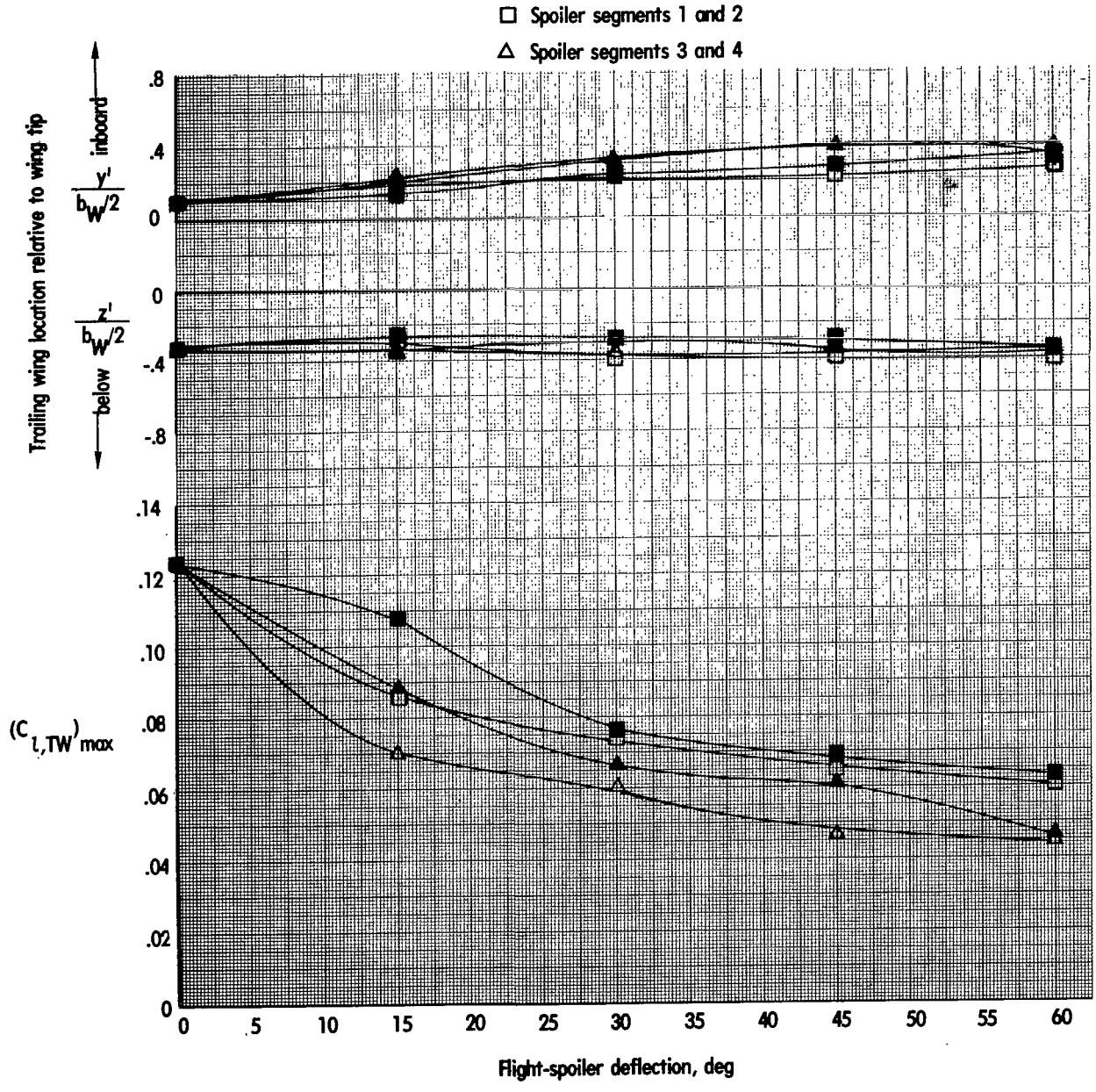

Figure 22.- Effect of simulating flight-spoiler segments with wedges on variation of trailing wing location and rolling-moment coefficient with flight-spoiler deflection for various segments of the flight spoilers. Trailing wing model located 9.2 transport wing spans behind transport airplane model; $C_{L,trim}$ = 1.2; landing flap configuration; landing gear down. Solid symbols indicate flight spoiler simulated with wedges.

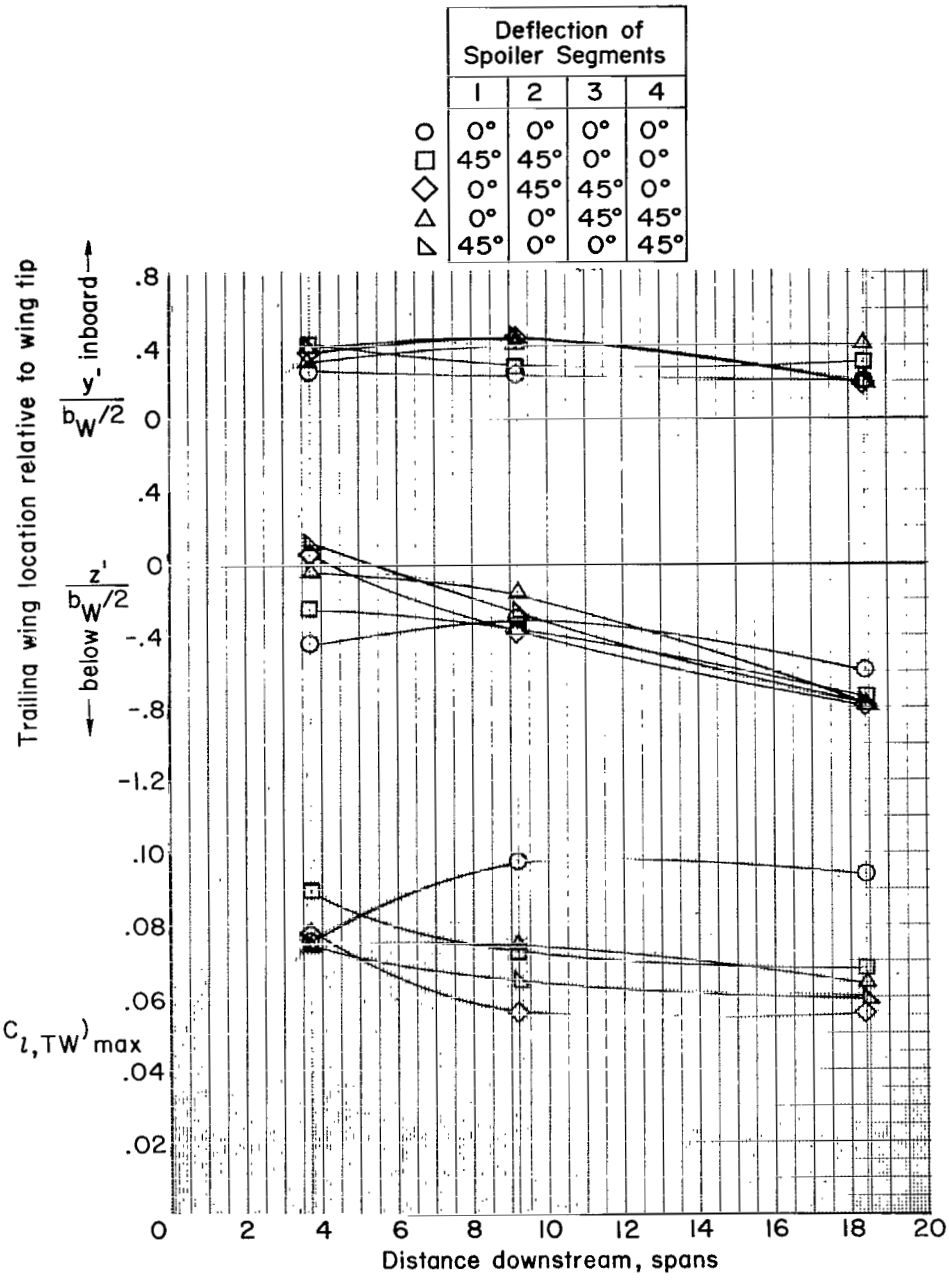

(a) Approach flap configuration; landing gear up.

Figure 23.- Variation of trailing wing location and rolling-moment coefficient with downstream distance behind transport airplane model (distance given in transport wing spans) with various segments of flight spoilers deflected 45°. $C_{L,trim} = 1.2$; flight-spoiler segment combinations of 2 and 3, and 1 and 4 simulated with wedges.

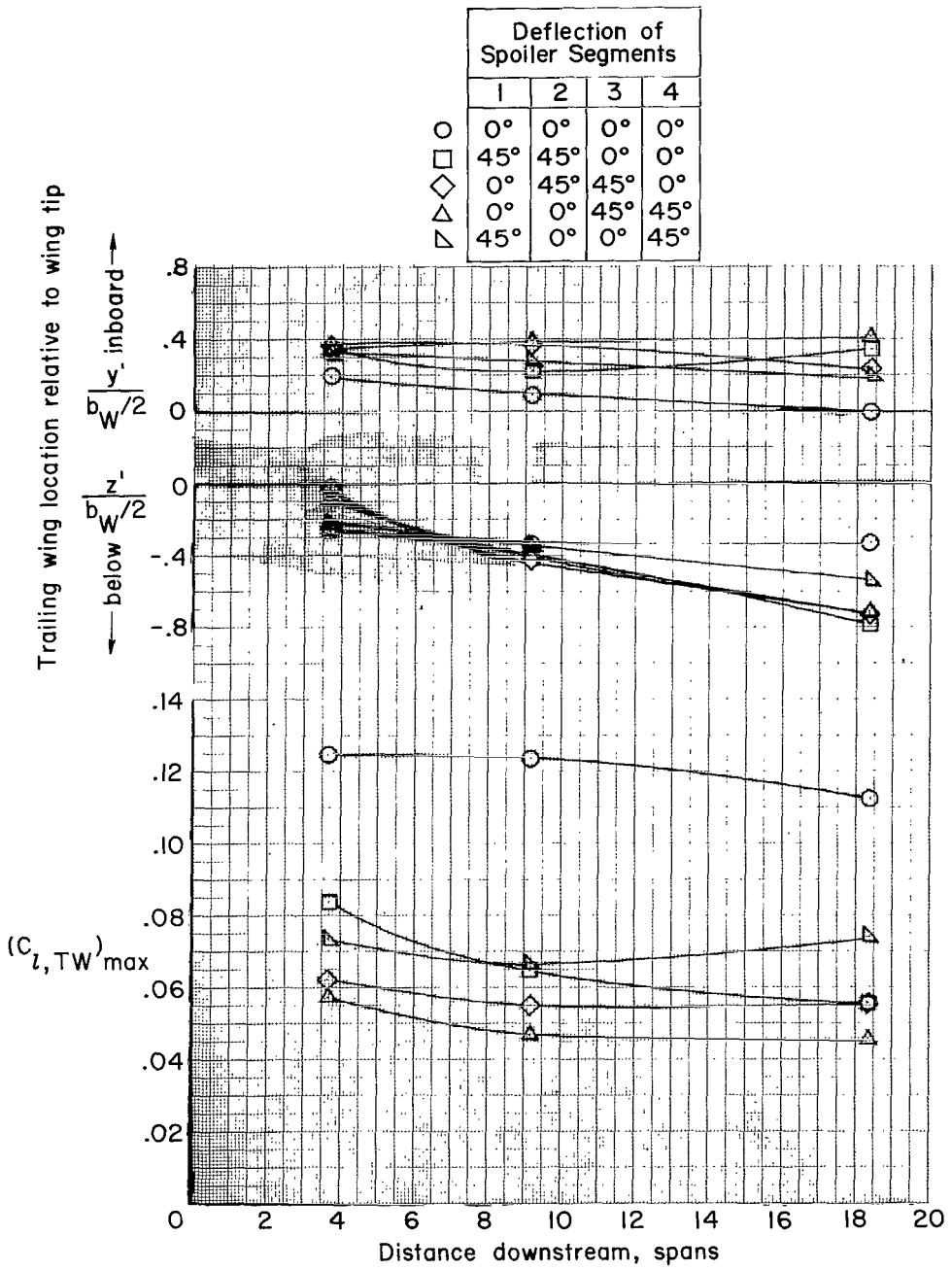

(b) Landing flap configuration; landing gear down.

Figure 23.- Concluded.

"The aeronautical and space activities of the United States shall be conducted so as to contribute . . . to the expansion of human knowledge of phenomena in the atmosphere and space. The Administration shall provide for the widest practicable and appropriate dissemination of information concerning its activities and the results thereof."

—NATIONAL AERONAUTICS AND SPACE ACT OF 1958

NASA SCIENTIFIC AND TECHNICAL PUBLICATIONS

TECHNICAL REPORTS: Scientific and technical information considered important, complete, and a lasting contribution to existing knowledge.

TECHNICAL NOTES: Information less broad in scope but nevertheless of importance as a contribution to existing knowledge.

TECHNICAL MEMORANDUMS: Information receiving limited distribution because of preliminary data, security classification, or other reasons. Also includes conference proceedings with either limited or unlimited distribution.

CONTRACTOR REPORTS: Scientific and technical information generated under a NASA contract or grant and considered an important contribution to existing knowledge.

TECHNICAL TRANSLATIONS: Information published in a foreign language considered to merit NASA distribution in English.

SPECIAL PUBLICATIONS: Information derived from or of value to NASA activities. Publications include final reports of major projects, monographs, data compilations, handbooks, sourcebooks, and special bibliographies.

TECHNOLOGY UTILIZATION PUBLICATIONS: Information on technology used by NASA that may be of particular interest in commercial and other non-aerospace applications. Publications include Tech Briefs, Technology Utilization Reports and Technology Surveys.

Details on the availability of these publications may be obtained from:

SCIENTIFIC AND TECHNICAL INFORMATION OFFICE

NATIONAL AERONAUTICS AND SPACE ADMINISTRATION

Washington, D.C. 20546